Fluid structure behaviour in gas-oil two-phase flow in a moderately large diameter vertical pipe

Rajab Omar [1], Buddhika Hewakandamby [1,*], Abdelwahid Azzi [2] and Barry Azzopardi [1]

[1] Faculty of Engineering, University of Nottingham, University Park, Nottingham NG7 2RD, United Kingdom

[2] Université des Sciences et de la Technologie Houari Boumedien, LTPMP/FGMGP, BP 32 El Alia, Algiers 16111, Algeria

Abstract

Intermittent flows in vertical pipes occur in many industrial settings including power generation and downstream oil-and gas production. This type of flows include cap bubble, slug and churn flow regimes. These regimes are of interest as downstream processes and control may heavily depend on the intermittency of the inflow. There are a number of correlations that predicts the features in such flows in vertical pipes. Most of the correlations were developed for air and water fluid pair for slug flow regime in vertical pipes with 25 to 50 mm inner diameter. In this paper, an attempt has been made to assess the suitability of several of these correlations specific to slug flow regime for a fluid pair that is different to air-water system. In this work, air-silicone oil flow development was experimentally investigated in a vertical pipe with an inner diameter of 68mm. A Wire Mesh Sensor (WMS) and an Electrical Capacitance Tomography (ECT) sensor were installed in series at four locations (15D, 30D, 45D and 65D) downstream of the mixing section. The flow was visually observed using a high speed camera. The void fraction time series obtained from the WMS and the ECT were used to establish the flow characteristics such as slug length, slug frequency, void fraction in liquid slugs and Taylor bubble velocity. A comparison showed that the void fraction measurements using ECT and WMS are in good agreement. Axial measurements shows that the flow development beyond 45D is minimal. Change in physical properties of the liquid phase is responsible for the

* Corresponding author. Tel.: +44 (0)115 9514178
E-mail address: buddhi@nottingham.ac.uk (Buddhi Hewakandamby).

deviation associated with the existing slug flow models, particularly those developed to predict the gas holdup in liquid slugs.

Keywords: Two-phase flow, slug flow, Electrical Capacitance Tomography, Wire Mesh Sensor, Flow development

1 Introduction

Situations where gas and liquid flowing simultaneously in vertical pipes are of importance to many process industries due to the flow patterns they produce depending on pipe diameters, flow rates and fluid properties. This poses a considerable challenge not only in designing such plants but also in controlling the processes. The intermittency in phases at the receiving end influences the choice of equipment as well as downstream process conditions. Over the time there have been many investigations focussed on developing robust models to predict the intermittent nature of gas liquid two phase flows (Khatib and Richardson, 1984; Barnea and Brauner, 1985; and Brauner and Ullmann, 2004). Most of the correlations were developed from data gathered using air and water as the fluids and pipe diameters around 25 or 38 mm pipes. This paper presents an attempt to assess the applicability of several of these correlations on larger pipe diameter with a liquid phase different to water.

Co-flowing gas and liquid in a pipe would arrange themselves depending on the flow rates, fluid properties and pipe geometries such as diameter and the inclination angle of the pipe. For the vertically upward flow, these configurations are mainly, bubbly, slug, churn and annular flows. Transition from one flow regime to another, which is due to the variation of the flow parameters and pipe layout geometry and the forces acting on the phases are of primary interest. Local measurements of flow parameter at different locations in co-current gas-liquid flow are desirable for development and validation of computational fluid dynamics (CFD) codes. Reliable two-phase flow data is required for developing flow models and confirming the existing models. The characterisation of axial flow evolution has a crucial industrial application, especially in gas and oil industry where the transition between flow patterns has a direct influence on the design of the downstream equipment.

Among the flow regimes, it is important to investigate the intermittent slug flow as it can cause severe damage to the installation. This is due the cyclic forces it could exert on the pipe and the structural supports that hold the pipes. In vertical upward flow, the intermittency appears as periodic units. Each unit is formed by a bullet gas bubble with a diameter almost equal to that of the pipe; the remaining space is filled with liquid. This bubble called Taylor bubble is followed by a small gas bubbles lying in the continuous liquid phase.

Since the early studies of Dumitrescu (1943) and Davies and Taylor (1950), a large volume of work, both experimental and numerical, has been carried out to analyse and characterize the slug flow regime (Taitel and Barnea, 1990; and Fabre, 2003). An analysis of the available literature shows that, with very few exceptions, all the investigations were achieved using air-water mixture and on laboratory size scale.

The models developed based on such data are devoid of the dependency on the physical properties of the process fluids used in many industrial settings. This has raised the demand of experiments that employ fluids with viscosity, density and surface tension different to that of water. Thereby the experiments presented in this work were designed to provide a more accurate and high-resolution database of measurements made utilising advanced instrumentations on an oil with physical properties close to that of industrial fluids. This data will expand the range of published results and could be used to evaluate the available flow transition models.

In this work, the axial flow development in 4.5 m long riser with 68 mm internal diameter (ID) is examined along with the characterisation of slug flow regime. The results describe how the flow structures in the vertical section develop as it moves downstream of the mixer. It also presents a detailed investigation of the axial flow development of slug flow. Air and 5 mPa.s

silicone oil experiments were conducted at ambient pressure and temperature for 60 different flow combinations.

2 Experimental arrangement and procedure

2.1 Flow facility description

The two-phase air-silicone oil flow experiments were conducted in the flow rig illustrated in Figure 1. The flow facility consists mainly of a liquid tank, a centrifugal pump, a mixing section, a vertical riser, a cyclone separator. Furthermore, air and liquid flow meters, electronic temperature sensors and pressure transmitters were implemented on the rig for measurements. The main Perspex pipe section has an average internal diameter of 68mm, while the air and the liquid inlets to the mixing section are 28 mm and 42 mm diameter respectively.

During the experiments, the silicone oil is pumped from the storage tank using the centrifugal pump into the mixing section. A bypass line is installed for a better liquid flow control and also to boost the flow stability. The air is supplied from a central compressed air line. Temperature and pressure of both the liquid and the gas streams are measured prior to the mixing section by electronic temperature sensors and pressure transmitters respectively. The silicone oil and air are well mixed within the mixing section and then the mixture flows along a vertical riser of 4.5 m length before it reaches the horizontal section. This offers 66 pipe diameter length which can be enough for the flow development (Azzi and Friedel, 2005; Benbella et al., 2009; and Abdulkadir et al., 2012). The two-phase flow in the vertical section is passed into the horizontal test section before it is returned to the holding tank where the phases are separated. The air is vented into the atmosphere while the silicone oil is returned to the bottom of the storage tank prior to its reuse.

The time series of the averaged void fraction was obtained at four different locations (15, 30, 45 and 65 pipe diameter) downstream of the mixer. The results of the first three locations were

mainly presented in this paper, since there was intangible change in the void fraction signal at 45 and 65 pipe diameter. For all experiments, the Wire Mesh Sensor (WMS) was placed immediately after the Electrical Capacitance Tomography (ECT) sensor to eliminate the impact of the intrusive nature of the former. It should be noted that the WMS is an intrusive technique that might cause distortion of the flow structures and bubble fragmentation, thus it is usually installed downstream of the non-intrusive ECT system.

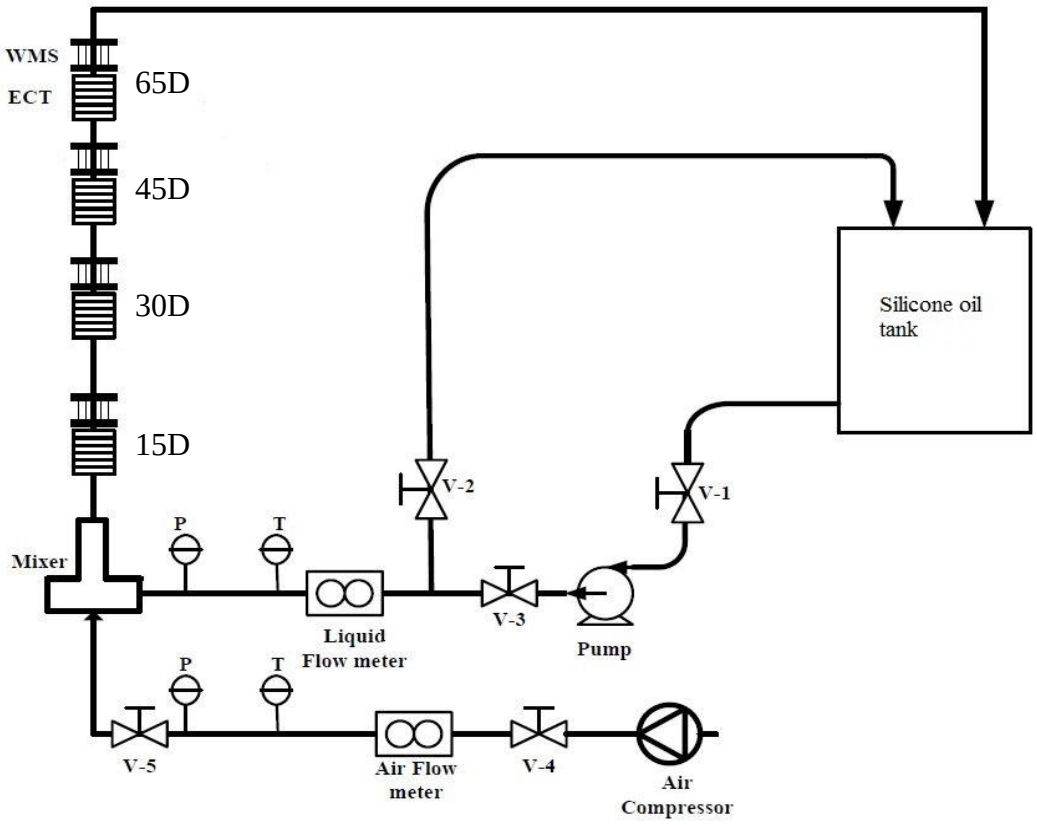

Figure 1: The schematic diagram of the flow facility.

2.2 Measurement techniques

Electrical Capacitance Tomography (ECT) which is described in detail by Hammer (1983) and Huang (1986) and the Wire Mesh Sensor tomography (WMS), that introduced by Prasser et al. (1998) and developed for capacitance measurement by Da Silva et al. (2007), were used to obtain real-time void fraction measurements in these experiments. These measurements

techniques have been extensively tested over the last decade and proved to be accurate within acceptable margins (Azzopardi et al., 2010; Sharaf et al., 2011; and Banowski et al., 2016).

To investigate the two-phase flow evolution, experiments are designed using ten gas superficial velocities in conjunction with six liquid phase superficial velocities giving a total of 60 conditions. The gas and liquid superficial velocities were varied from 0.045 to 3.2 m s^{-1} and from 0.15 to 0.53 m s^{-1} respectively. A data acquisition system using LabVIEW software was developed for simultaneous acquisition of data from all devices. A trigger signal from the WMS is used to initialise the ECT and the other measuring devices including flowmeters.

During each experiment, the flow rate, pressure, temperature and void fraction were measured after allowing the flow to stabilise. The process was repeated for each run until the full set of experiments was completed.

The consistency of the results was checked through data analysis process which included computing the probability density functions (PDF), frequency and structure velocities.

Detailed analysis of the void fraction time series signal (as described in section 3) was performed. The characteristic parameters are reported including, cross-sectional averaged void fraction, probability density functions, structure frequency and velocity, slug length, Taylor bubble velocity, and the void fraction in the body of slugs. The available flow models and existing empirical correlations were tested using the experimental data at 45D downstream of the mixer, where the flow is considered developed.

3 Data processing

The instrumentations that were used in this work such as capacitance WMS and ECT system offer a wide range of detailed information on the two-phase flow structure at various locations

along the vertical pipe. Real-time measurements in the form of void fraction time series were obtained from both sensors.

The obtained voltage signals from WMS and ECT system were converted to void fraction data utilising a calibration routine. The time series of the void fraction distribution was used to estimate several flow parameters including the probability density functions (PDFs), radial void fraction, bubble size distribution, structure frequency and structure velocity.

3.1 Probability density function

Probability density functions (PDF) shows how often each value of void fraction occurs within a particular range. PDFs plots show the rate of change of probability with void fraction values, where the total area under PDFs plot should be equal to one. The PDFs has been widely used to identify the relevance flow patterns. The work of Jones and Zuber (1975) demonstrates the ability of this statistical property to discriminate between the main flow patterns. In addition, PDFs can also be used to estimate different flow parameters such as film thickness, slug length and bubble length in slug flow (Costigan and Whalley, 1997).

The PDFs plots of the cross-sectional averaged void fraction are used to categorise the corresponding flow patterns based on the work of Jones and Zuber (1975) and Costigan and Whalley (1997) in which they pointed out that the PDFs of the void fraction data can be used to quantitatively discriminate the main flow patterns. Bubbly flow is associated with a single peak at low void fraction, while a broad single peak at high void fraction and a tail stretched to low void fraction represents churn flow. Slug flow, the intermittent flow pattern between bubbly and churn flow, is identified by a twin peak PDF, one at low void fraction corresponding to the void fraction in liquid slug and the other at high void fraction representing Taylor bubble.

The PDF of the cross-sectional averaged void fraction was computed by taking into account the occurrence frequency of the void fractions within the population collected during the

measurement period. For this paper, we have considered 100 bins between 0 and 1 for the void fraction data.

3.2 Structure Frequency

The power spectral density (PSD) method was applied to obtain the frequency of the time series data that describe the periodicity of the flow structures such as slugs. The PSD was estimated through discrete Fourier transform of the autocorrelation of the time series. Fourier analysis transforms the void fraction data form its time domain to the frequency domain as shown in equation **Error! Reference source not found.**.

$$S_{xx}(f) = \int_{-\infty}^{+\infty} R_{xx}(\tau) e^{-j2\pi f\tau} d\tau \qquad (1)$$

where; R_{xx} is the autocorrelation function of the void fraction time series while $S_{xx}(f)$ is the power spectral density as reported by Bendat and Piersol (1980).

The frequency of the structures was also estimated using the method proposed by Hazuku et al. (2008) for large disturbance waves. The void fraction signal from the WMS and ECT was used to estimate the front and the tail of Taylor bubble. A Taylor bubble is defined as a part of the void fraction signal whose peak is higher than the upper average of the void fraction and both ends are lower than the average of the void fraction as described by Hazuku et al. (2008). The part of the signal between two trailing Taylor bubbles represents liquid slug. The results were in a good agreement with the manual counting and the PSD method.

3.3 Structure velocity

The structure velocity was determined by cross correlating the void fraction time series obtained from the twin-plane ECT sensor. Cross correlation function is simply the sliding dot product of the two time series from the two ECT planes to estimate the time delay τ between them as shown in the equation **Error! Reference source not found.**. In this case *x* and *y*

represent the signal at the first and second plane of the ECT system respectively. Thus the cross-correlation is given by

$$R_{xy}(t, t+\tau) = \frac{1}{N} \sum_{i=1}^{N} x(t_i) y(t_i + \tau) \quad (2)$$

where N is the number of samples in each time series. It produces the time delay of a signal which is equal to the distance divided by the propagation velocity. Since the distance between the planes of the sensors is known, the structure velocity is merely equal to the distance between the two sensors divided by the time delay estimated from the cross-correlation.

3.4 Slug length

The length of slugs was estimated using the averaged transitional velocity of slugs and the resident time of slugs at the measuring plane. The velocity was assumed to be constant throughout the test section and the following equation was used to determine the slug length.

$$L_s = \Delta_t \, . \, U_s \quad (3)$$

Where; L_s is the slug length, Δ_t is the resident time of slugs at the sensor and U_s is the velocity of slugs.

All mathematical operations are implemented in MATLAB, is some cases, using embedded routines within the software.

4 Results and discussion

4.1 Comparison between WMS and ECT performance

Electrical Capacitance Tomography (ECT) and Wire Mesh Sensor (WMS) tomography have been widely tested for multiphase flow applications over the last decade. For instance WMS measurements showed good agreement with X-ray tomography and Gamma radiography for void fraction measurements as reported by Prasser et al. (2005) and Prasser (2000). Whereas Azzopardi et al. (2010) concluded that the ECT and WMS give a similar mean void fraction,

they also highlighted the advantage of each technique. For all experiments reported in this work, the WMS was placed downstream of the ECT sensor in order to minimise the intrusive nature of the WMS and also to limit the change in the vertical distribution of the void fraction between the two measuring planes.

The void fraction data gathered from both sensors showed a reasonable agreement for all experiments. Figure 2 shows PDFs of the cross section averaged void fraction time series data simultaneously collected using WMS and ECT at the given flow conditions. The comparison illustrates that at liquid superficial velocity, U_{ls}, 0.22 m s^{-1} and gas superficial velocities, U_{gs}, 0.045 m s^{-1} and 0.18 m s^{-1}, the PDF corresponds to bubbly flow (Figure 2-a) and cap bubble (Figure 2-b) respectively. For these flow patterns, the WMS seems to give higher void fraction which might be due to the drag effects triggered by the intrusive nature of the sensor, where at low flow rates the bubbles decelerate at the measuring plane causing an increase in average void fraction.

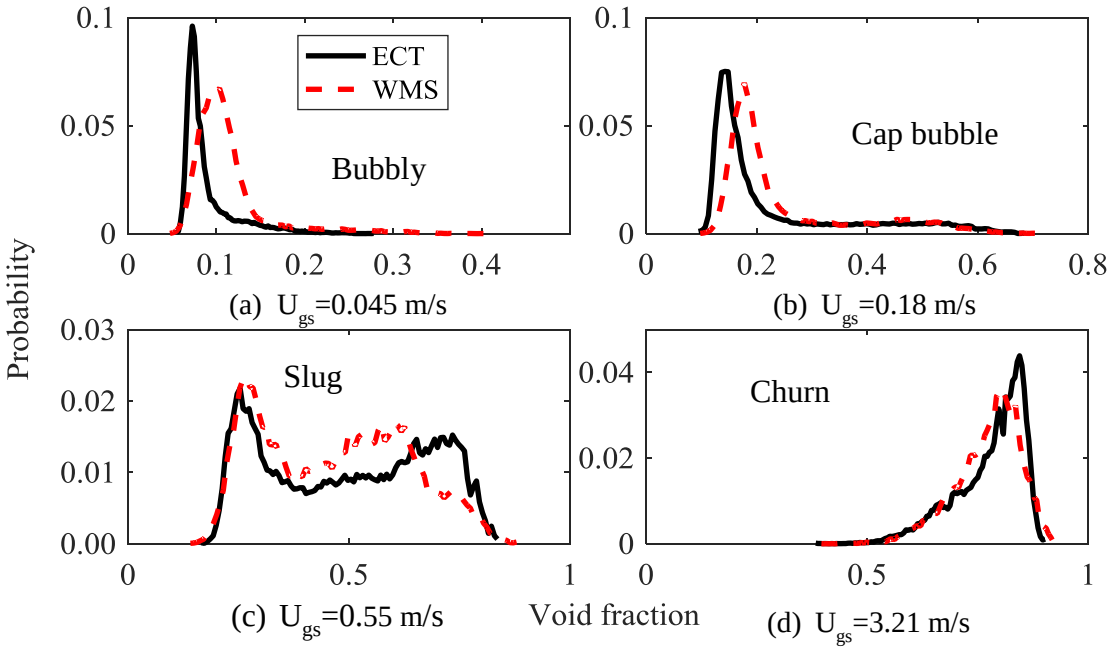

Figure 2: PDF plots of the cross-sectional averaged void fraction for ECT and WMS at 45 ID downstream the mixer. The liquid superficial velocity = 0.22 m s^{-1}.

At gas superficial velocity, U_{gs} 0.55m s^{-1} (Figure 2-c), both sensors show almost similar PDF plots which indicate slug flow. For the maximum flow condition achievable in these experiments (U_{ls}=0. 22m s^{-1}, U_{gs}=3.21m s^{-1}) (Figure 2-d), the PDF signatures for ECT and WMS characterise churn flow, where ECT provides a higher peak at slightly higher void fraction than the WMS. It is obvious that the difference between the PDF plots created using the two sensors reduces as the gas superficial velocity increases. Generally, the PDF signature for both devices indicates similar flow patterns. The results showed a good agreement between both sensors, for the full range of flow conditions, with an average percentage error of 5% and standard deviation of 1.02, while the averaged absolute percentage error is 6.7% in void fraction measurements.

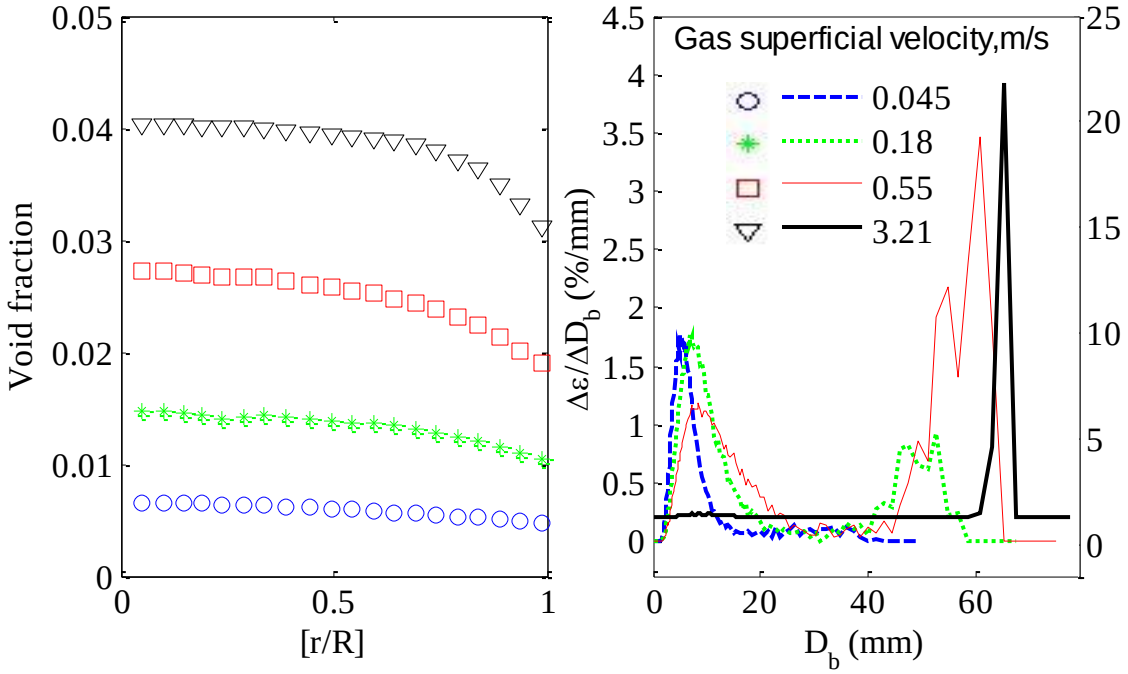

a. Radial void fraction b. Radial void fraction

Figure 3: Radial void fraction profile and bubble size distribution obtained from WMS at 45D downstream of the mixer. Liquid superficial velocity = 0.22 m.s^{-1}.

The radial void fraction profiles and bubble size distributions at different gas superficial velocities are illustrated in Figure 3. The radial distribution of gas fraction shows a flat profile

at low gas superficial velocity (U_{gs}=0.045 m s^{-1}). This corresponds to a dispersed bubbly flow, in which small gas bubbles are uniformly distributed throughout the cross section of the pipe. As the gas superficial velocity increases, the uniform distribution disappear and the radial void profile tends to indicate a local maxima at the core of the pipe. At these conditions large bubbles are formed and rapidly shifted to the centre of the pipe. At U_{gs} = 0.18 m s^{-1} and 0.55 m s^{-1} the bubble size distribution switched from single to bimodal, indicating the transition to cap bubble and slug flow regime respectively. The most significant observation from these results is that the bubble sizes at the measuring plane are greater than the wire spacing of the WMS and hence the error due to the sub-resolution bubble sizes is considered to be minimum. This is expected since the initial bubble size is 3mm while the spatial resolution of the sensor is 2.8 mm. It seems that small bubbles are deaccelerated at the sensor wires while the large bubbles are accelerated as reported by Ito et al. (2011). This hypothesis explains the reduction in the difference between the two sensors as the gas superficial velocity increases.

Banowski et al. (2016) suggested the best working range for the WMS. They also reported that the sensor insensitiveness of small bubbles could be overcompensated by the deceleration of bubbles at the crossing point. Therefore, in this case, the WMS is expected to overestimate the averaged void fraction at a low gas flow rate. On the other hand, the limited spatial resolution of the ECT sensor should not be ignored. It is a non-invasive sensor and hence the void fraction at the core of the pipe may not be accurately represented, especially when the gas phase is not uniformly distributed. On the other hand, a twin plane ECT system can provide velocity information without altering the flow structure.

In conclusion, it can be said that both sensors can give an acceptable and comparable estimation of the cross-sectional average void fraction. The high temporal and spatial resolution of the WMS in comparison to ECT sensor can provide detailed information of the flow and can detect bubbles within its spatial resolution. The dual plane ECT sensor offers the prediction of the

structure velocity without disturbance of the flow. Both sensors have strengths and weaknesses due to the limitations in their respective designs and it is difficult to select one over the other. It is obvious that if both sensors are integrated, a considerable amount of flow information can be obtained.

4.2 Cross-sectional averaged void fraction

Figure 4 illustrates the cross-sectional averaged void fraction at U_{ls} = 0.3 m s^{-1} at four axial locations along the test section. It should be noted that the difference in averaged void fraction at 45D and 65D is small and within the uncertainty margin for the measurements. The PDF plots at 45D and 65D are identical in shape and no change in the flow structures was observed. Therefore, the changes due to flow development are considered to be insignificant at those locations.

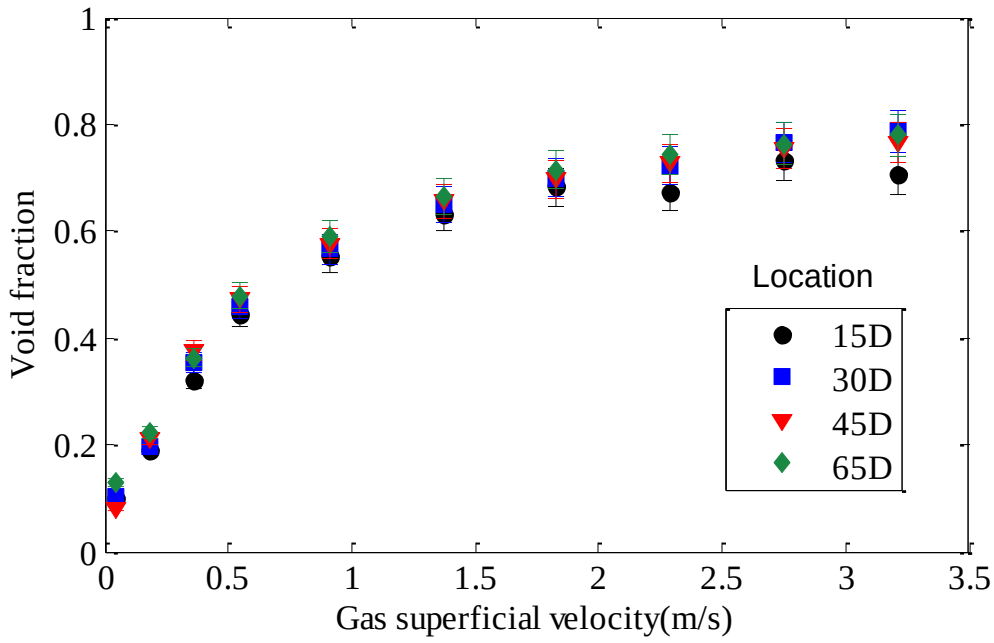

Figure 4: Mean void fraction at four axial locations at liquid superficial velocity, U_{ls} = 0.3 m s^{-1}.

The superficial gas velocity has a significant influence on the subsequent flow development in the riser. Figure 5 shows the mean void fraction for the range of gas and liquid flow rates 45D downstream of the gas injection point. The curves indicate a continuous increase in the void

fraction with increasing superficial gas velocity. It can be seen that the void fraction is sensitive to the change of superficial gas velocity at low values. Figure 5 clearly indicates that the curves tend to level off beyond the superficial gas velocity 1.5 m s^{-1}. This trend can be interpreted as the change in flow patterns with the increase of superficial gas velocity. The transition from bubbly to slug flow is associated with a considerable shift in the rate of change of the void fraction, w.r.t. the superficial gas velocity. The higher gradient up to U_{gs} = 0.55 m s^{-1} explains bubbly flow, whereas the transition from slug to churn incorporates a slight change in the rate of change of void fraction beyond U_{gs} > 0.91 m s^{-1}.

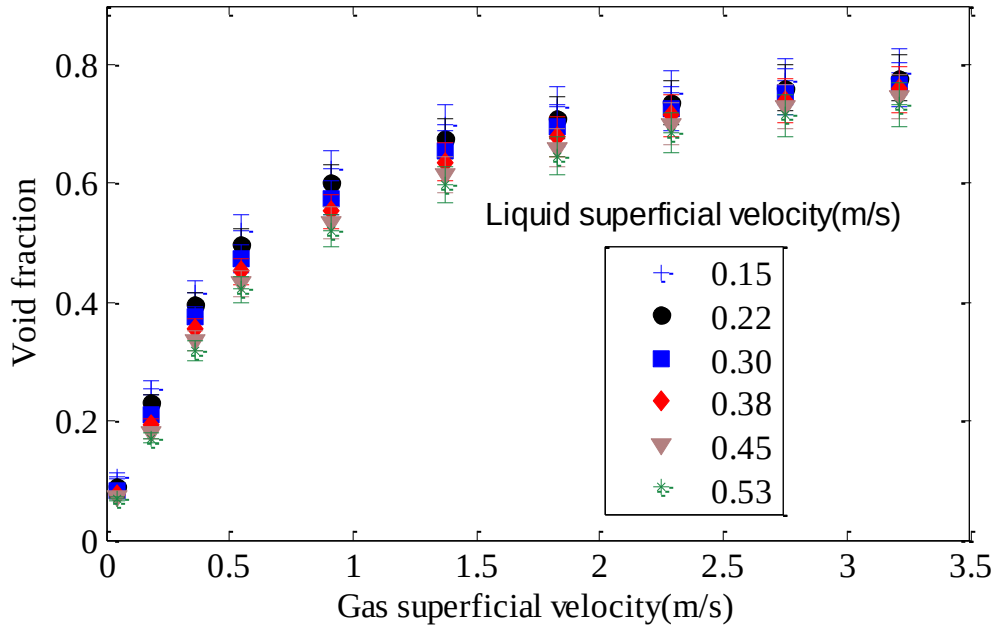

Figure 5: Variation of the averaged void fraction with superficial gas velocity for several liquid superficial velocities at 45D.

The influence of superficial liquid velocity on the mean void fraction shows a decrease in the void fraction as the liquid superficial velocity increases. However, it can be mentioned that the superficial liquid velocity has a weak influence on the void fraction comparing to that of superficial gas velocity.

4.2.1 Void fraction estimation

Void fraction is a crucial parameter in characterising two-phase flow. Therefore an accurate prediction of void fraction is of great interest in industrial applications. In this work, Drift-flux model was used to estimate the void fraction in the region of slug flow. Drift-flux model considers the mixture as whole, instead the two-phase separately. The one-dimensional drift-flux model, that was introduced by Zuber and Findlay (1965) and developed by Wallis (1969) and Ishii (1977), is widely used to estimate the averaged void fraction. It is usually preferred over the two-fluid models for its simplicity and applicability in a wide range of flow conditions. The general form of the one-dimensional drift-flux model is represented by equation **Error! Reference source not found..**

$$\varepsilon_d = \frac{U_{gs}}{C_0 U_m + U_d} \tag{4}$$

Average void fraction is given by $\varepsilon_d$while U_d and C_0 are the drift velocity and distribution parameter respectively. The drift velocity is the relative velocity between the gas phase and mixture velocity at the centreline. The distribution parameter represents the relative velocity of the gas phase in Taylor bubble to the mixture velocity of slug unit. The drift velocity is estimated by the equation proposed experimentally by Nicklin et al. (1962) which is given by the equation **Error! Reference source not found.** which is in agreement with the theoretical work of Dumitrescu (1943) and Davies and Taylor (1950).

$$U_d = 0.35\sqrt{gD} \tag{5}$$

where g is the gravitational constant and D is the internal diameter of the pipe. The distribution parameter C_0 was found to have different values with respect to the corresponding flow patterns. For slug flow it is widely acceptable that C_0 is equal to 1.2, however in this work the equation proposed by Hibiki and Ishii (2003), that accounts for density differences, is used.

$$C_0 = \left(1.2 - 0.2\sqrt{\frac{\rho_g}{\rho_l}}\right) \quad (6)$$

The symbols ρ_g and ρ_g represent the density of gas and liquid respectively. The Drift-flux model results were compared to the experimentally measured averaged void fractions at 15D, 45D, and 65D downstream of the mixing section as presented in Figure 6. The predicted void fraction at 45D and 65D is almost identical. The figure shows a reasonable agreement between the predicted and experimental data with an average percentage error of -2.38 and standard deviation of 0.6. The accuracy of the model decreases for data obtain closer to the mixing section. For instance, at 15D, the cross-sectional void fraction data was visibly under predicted with an average percentage error of -8.5 and standard deviation of 0.6. It is evident that highly aerated underdeveloped slugs were more dominant at 15D from the mixing section leading to underestimation of the void fraction. As the slugs move upward towards 45D and 65D downstream of the mixer, developed slugs become more frequent leading to improved accuracy of the predicted data. Since the change in the averaged void fraction and the flow structure at 45D and 65 D was insignificant, and also there is no recognisable difference in the flow structures at 45D and 65 D, The flow is considered as developed at 45D and beyond. Therefore, to minimise the number of experiments and to minimize the experimental costs, measurements were made only up to 45D in this campaign.

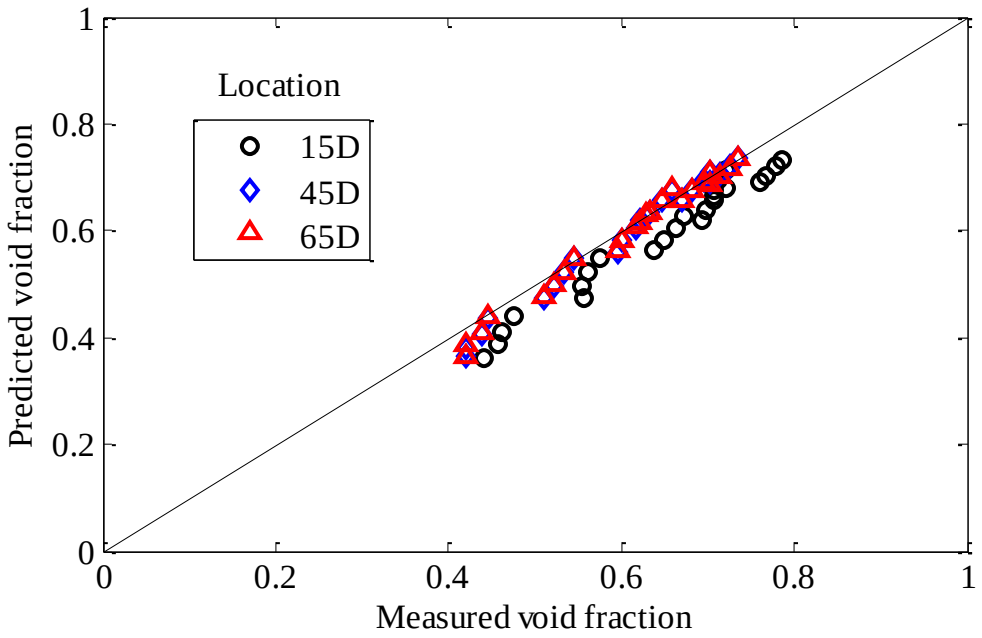

Figure 6: Comparison of experimentally measured void fraction and predicted void fraction using drift flux model at 15D and 45D downstream of the mixer.

4.3 Flow patterns identification

The PDF signatures of the cross-sectional averaged void fraction, obtained from the WMS and ECT, are used to identify the corresponding flow patterns. Visual observations corroborated the statistical analysis and have been widely used to discriminate the main flow patterns qualitatively. The main flow patterns observed in the riser are bubbly, cap bubbles, slug and churn. Figure 7 shows the time series of the main flow pattern and their PDFs for gas superficial velocity ranges from 0.45 to 3.21 $m.s^{-1}$ and liquid superficial velocities from 0.15 to 0.53 $m.s^{-1}$. The results show that each flow regime has a unique probability density function distribution comparable to those reported in the literature.

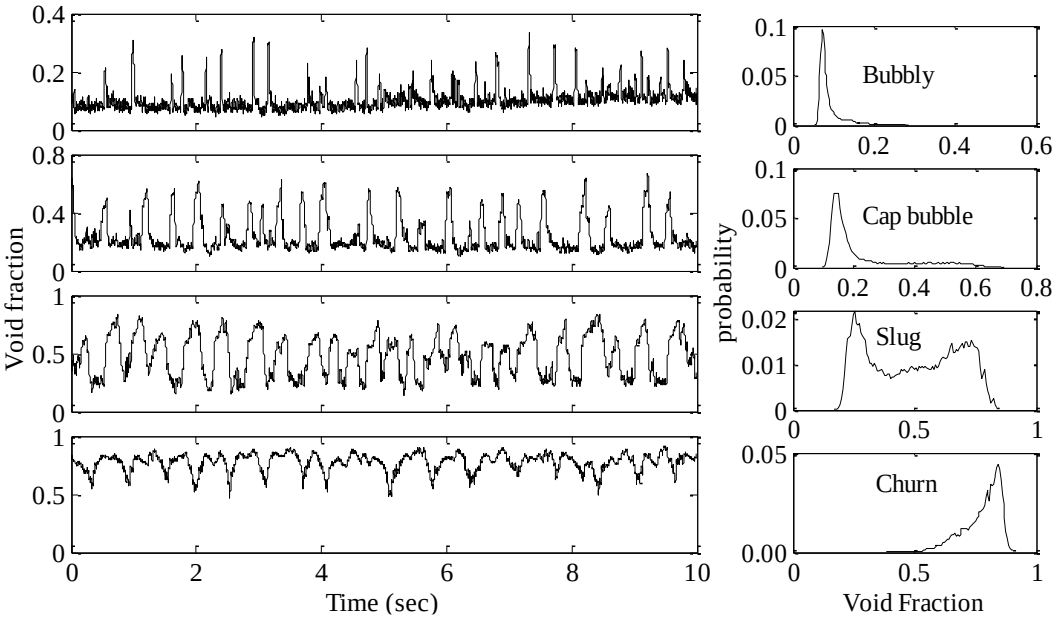

Figure 7: Cross-sectional averaged time series of void fraction and the corresponding PDFs for each flow pattern.

According to Costigan and Whalley (1997), slug flow is identified by twin peak PDF, one at low void fraction corresponding to the smaller bubbles in the liquid slug, while the other at high void fraction corresponding to the Taylor bubble. The most remarkable observation in the riser was the non-developed slugs; they are short and highly aerated slugs, similar to those reported by Nydal et al. (1992) in horizontal pipes. Non-developed slugs in the riser are more likely to occur near the transition to churn flow at high gas flow rates. This type of slug is characterised by a single wide peaked PDF. Therefore it can be inaccurately identified as churn flow. Figure 8 illustrates the difference between developed slugs and non-developed slugs.

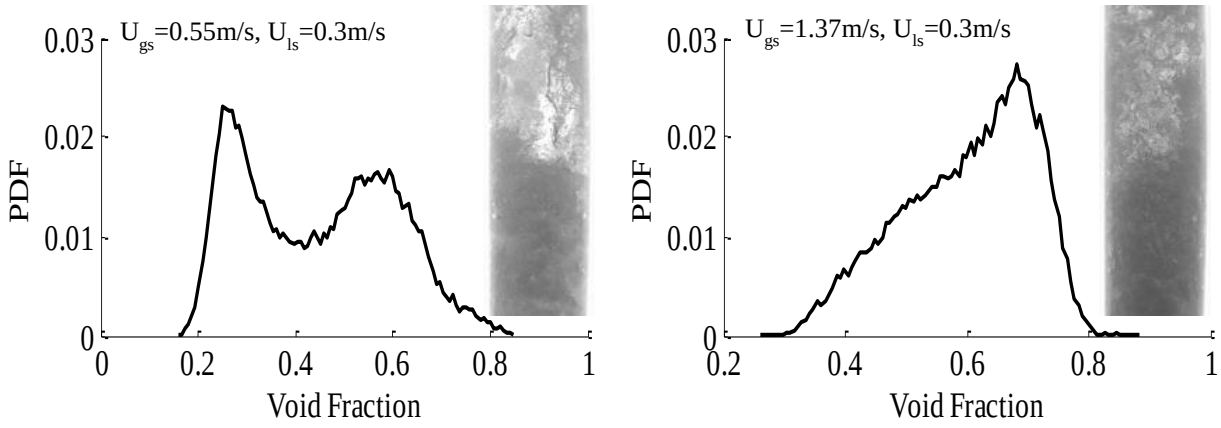

a. Developed slug

b. Non-developed slug

Figure 8**: Probability density function of a developed slug and a non-developed slug.**

4.4 Flow transition along the axial direction

Void fraction measurements at three different locations downstream of the mixing section were conducted. Void fraction information at each location is obtained using the ECT and the WMS measurement probes.

It can be seen from Figure 9 that at lowest gas superficial velocity (case (a)), the averaged void fraction near the mixer (at 15D) is the highest, while at the second location, 30D, it records the lowest void fraction before increasing again at 45D downstream the mixer. Since the PDF plots, as well as the visual observation, indicate bubbly and cap bubble flow, it can be reasoned that at low gas superficial velocity, finer bubbles form near the mixer resulting dispersed bubbly flow. Furthermore, the bubble density is high making the mixture to appear like a foam. As the bubbles move up to the second position, 30D, larger ellipsoidal bubbles formed due to coalescence and these bubbles moves to the centre of the pipe occupying a smaller area of the cross section of the pipe. The observation is in agreement with Prasser et al. (2002) and Lucas et al. (2005) for multi-disperse bubbles and Tomiyama (1998) for a single bubble. As the large bubbles move upward at relatively higher velocity, more coalescence occurs forming larger cap bubbles and hence the void fraction increases again.

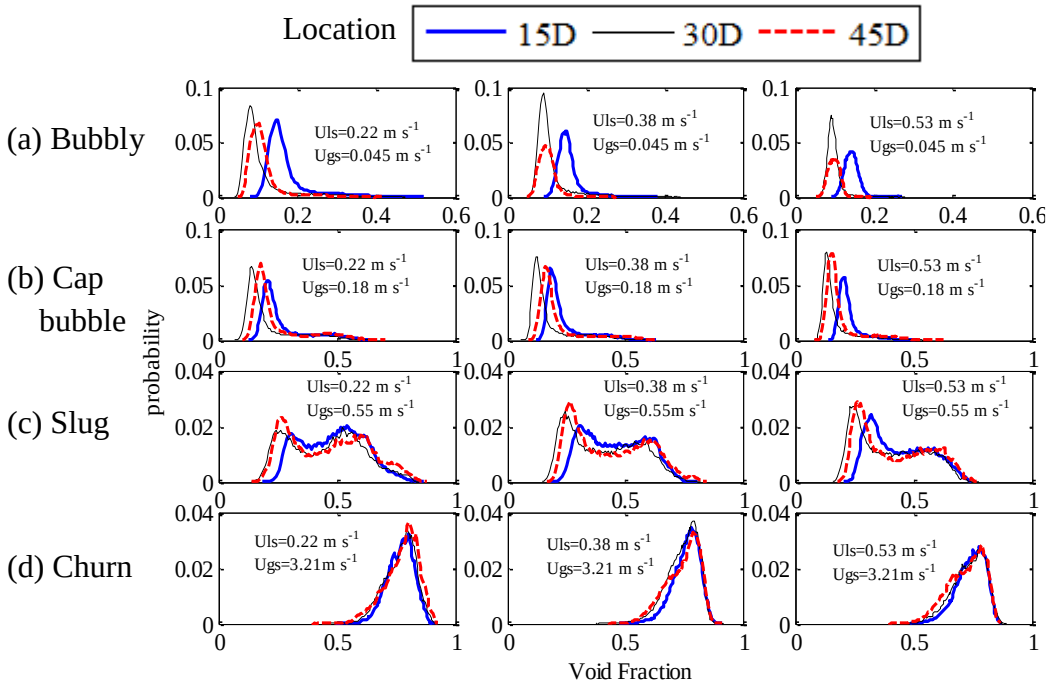

Figure 9: PDF plots for different flow condition at 15D, 30D and 45D downstream the mixer.

PDF plots were generated for superficial gas velocities 0.045 m s^{-1}, 0.18 m s^{-1}, 0.55 m s^{-1}, and 3.21 m s^{-1} and superficial liquid velocities 0.22 m s^{-1}, 0.38 m s^{-1}, 0.53 m s^{-1} at selected axial positions. The flow pattern changes with different combinations of the liquid and gas superficial velocities as shown in Figure 9 (a-d). Several flow patterns such as bubbly (Figure 6-a), cap bubbles (Figure 6-b), slug (Figure6-c) and churn (Figure 6-d) could be attained in the riser. As the gas superficial velocity increases, the PDFs produced for the three measurement locations are almost similar. It seems that at high gas flow rates, the change in the averaged void fraction along the axial length is insignificant thus the required length for flow development is expected to be shorter under these conditions. However, the interaction between phases is considered to continue in risers, regardless their length, due to the change in pressure and forces acting on bubbles.

4.4.1 Bubble size distribution and radial void fraction

Bubble size distribution is obtained from WMS data using the algorithm developed by Prasser et al. (2001). It is based on the gas volume fraction contained in each class of bubbles instead of the number of bubbles. Figure 10 illustrates the bubble size distribution at three different flow conditions. The x-axis denotes the volume equivalent bubble diameter (D_b) and the y-axis denotes the ratio of the gas fraction per bubble class ($\Delta\varepsilon$) to the equivalent diameter of the bubble class (ΔD_b).

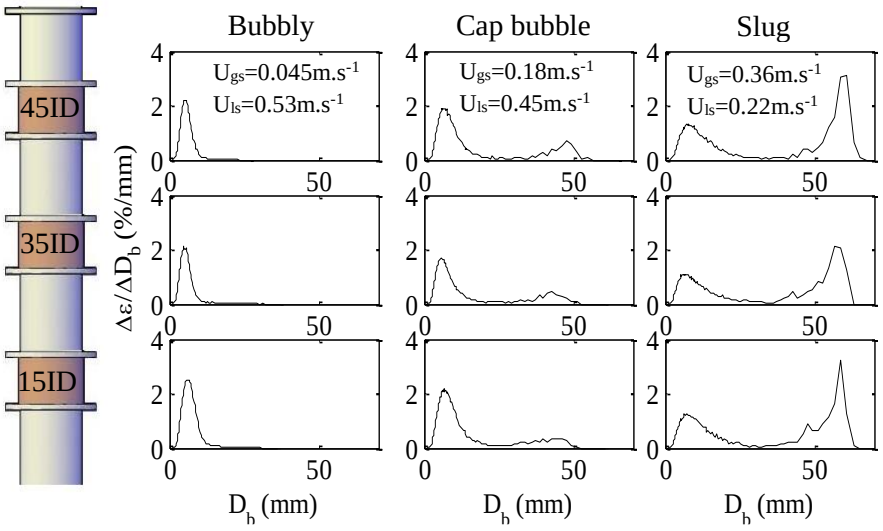

Figure 10: Bubble size distribution for different flow patterns at three axial locations along the test section.

It is obvious that in the bubbly flow region the distribution displays a single peak at small bubble size, this peak is shifted to the right as the bubbles move upwards in the column indicating the bubble coalescence. At bubble/cap bubble transition, the distribution for the first location shows a single peak indicating small bubble sizes and a long tail extended to relatively large bubble sizes. This represents a nonhomogeneous bubbly flow. As the flow develops in the axial direction, a second peak becomes apparent. This peak shows that large cap bubbles become more frequent. It is clear that the estimated diameter of these bubbles is around 50 mm, slightly below the pipe diameter. In slug flow region, the bubble size distribution is

characterised by double peaks; one at small bubble size, similar to that of bubbly flow, and the other for bubble diameters equivalent to the size of the pipe representing Taylor bubbles. Similar to PDFs, it is possible to use the bubble size distribution to discriminate between flow patterns such as bubbly (disperse/cap bubbles) and slug flow. However, bubble size distribution does not provide discrimination for the transition from slug to churn flow since both regimes are represented by a dual peak distribution. There is usually an agreement between the bubble size distribution and PDFs results, both plots could give a clearer image of the axial evolution of the flow.

4.5 Slug Unit Characterisation

A slug unit consists of an elongated bubble called Taylor bubble followed by a liquid slug which usually contains dispersed bubbles. In this work, a distorted gas bubble was observed; which is the case for relatively large diameter pipes as shown in Figure 11.

Figure 11 indicates that slug like structures can be observed in relatively large diameter pipes. The only difference is that instead of bullet shape Taylor bubble, a distorted large gas structure forms the part of the periodic slug unit.

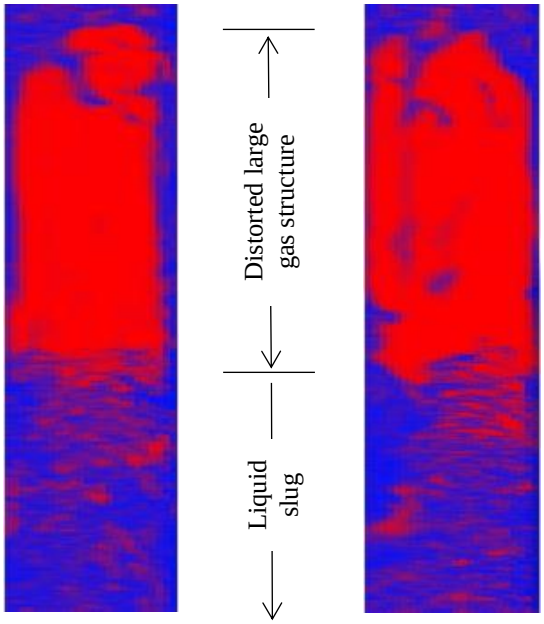

Figure 11: Cross-sectional images obtained from the WMS for slug flow structure.

One dimensional model is commonly used to model slug flow, in which the slug phenomenon is simplified to a sequence of identical units flowing at constant velocity (Wallis, 1969; Fernandes et al., 1983; and Taitel and Barnea, 1990). Due to the intermittency of the slugging phenomenon, the estimation of slug characteristics, such as slug frequency and the length, is a crucial factor for industrial design and operation. For instance, the maximum length of liquid slugs is important for the design of slug catchers and two-phase separators. These flow characteristics vary in time and space, therefore several correlations were proposed in order to predict the main features of slugs in vertical pipes, such as Taylor bubble velocity, gas hold up within the body of liquid slugs, length of liquid slugs and the frequency of slugs (Nicklin et al., 1962; Sylvester, 1987; Khatib and Richardson, 1984; and Legius et al., 1997).

In the following subsections, the development of slug flow is investigated; the effects of superficial gas velocity and axial flow position are examined. The experimental results were compared to the available correlations, which are originally proposed for fully developed flow.

4.5.1 Slug length

Slugs consist of two parts; the Taylor bubble and the liquid slug. The length of liquid slugs was estimated using the averaged transitional velocity and the resident time of the liquid slugs at the measurement plane as explained in Section 3. Figure 12 shows the axial development of the averaged liquid slug length at three different locations in the riser. It can be clearly seen that the averaged liquid slug length increases along the pipe. The rate of increase in liquid slug length is smaller near the pipe exit and at high gas superficial velocities. This increase of the liquid slug length in the axial direction is due to the coalescence of Taylor bubbles. At the first location (15D) the slugs are not fully developed, and the distance between consecutive Taylor bubbles is small. The trailing bubble is influenced by the flow within the preceding liquid slug. As a result, the trailing bubble travels faster than the leading bubble and as a consequence, the rate of slug growth is higher around this location. As the liquid slugs move further upward, the merging process decreases due to the increase in the length of liquid slugs. At 45D, the length of liquid slugs is almost double the size of the slugs at 15D downstream of the mixing section. This indicates clearly the coalescence of slug units. It can be stated that near 45D, the slugs are almost developed, regardless the infrequent observation of short slugs. However, it could be argued that the merging process may continue in extremely long pipes, due to the energy dissipation and pressure difference.

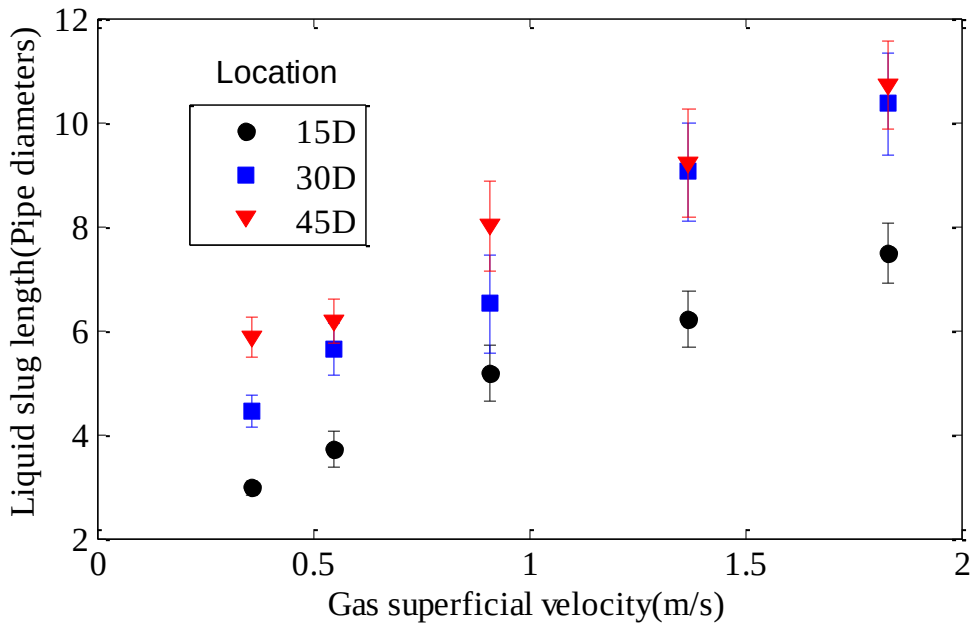

Figure 12: The axial development of the mean liquid slug length in the riser at liquid superficial velocity = 0.3 ms^{-1}.

It was observed that the length of slugs and Taylor bubbles increase with the increase of superficial gas velocity as shown in Figure 13. The slug length, at 45D downstream of the mixing section, was found to vary between 6D and 12D. This is still within the range of the reported minimum stable slug length, about 8 to 16 D (Moissis and Griffith, 1962; Taitel et al., 1980).

Slug length correlation developed by Khatib and Richardson (1984) was used to estimate the experimental results of slug lengths as given in Equation **Error! Reference source not found.**. The predicted slug length was in an acceptable agreement with experimental data as shown in Figure 14.

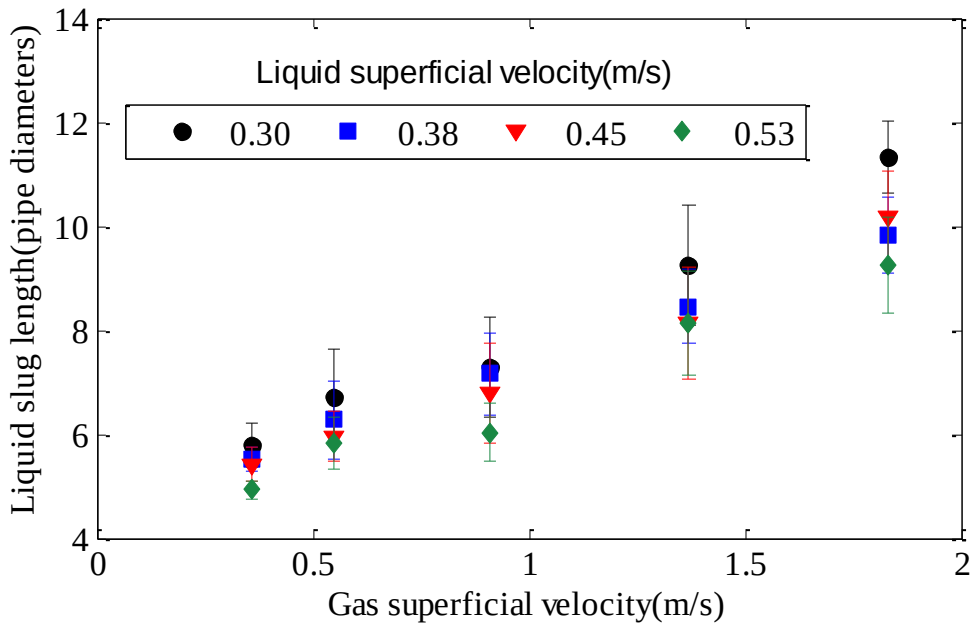

Figure 13: Liquid slug variation at different flow conditions.

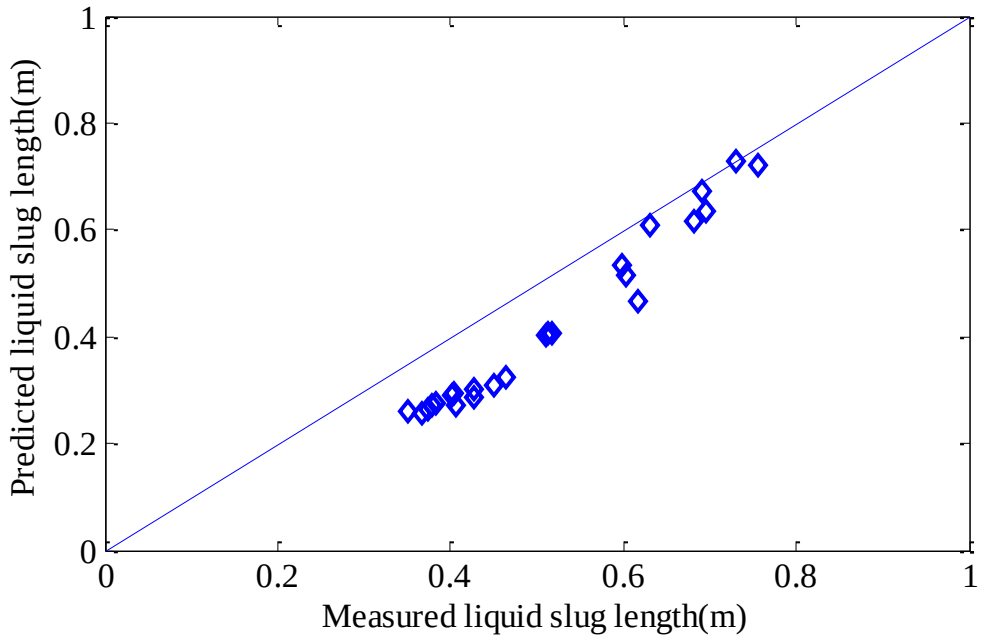

Figure 14: Comparison of experimentally measured slug length and predicted slug length using Khatib and Richardson (1984) correlation.

It is clear from Figure 14 that Khatib and Richardson correlation slightly underpredicts the mean length of the slug body, especially at low gas superficial velocities. The whole data was predicted with an average absolute error of 20.70% and standard deviation of 1.92.

Khatib and Richardson correlation is given by

$$L_S = \frac{C_0 U_m + U_0}{f_S}\left[\frac{\varepsilon - \varepsilon_{gTB}}{\varepsilon_{gsl} - \varepsilon_{gTB}}\right] \quad (7)$$

where U_m is the mixture velocities, f_S is the slug frequency ε is the averaged void fraction, the ε_{gsl} void fraction in liquid slug, and ε_{gTB} Void fraction in Taylor bubble. The discrepancy between the experimental and predicted values could be attributed to the assumptions made by Khatib and Richardson (1984). The correlation was proposed through a simple mass balance around a slug unit, in which the slug unit was assumed to travel at a constant velocity. The effect of physical properties was not included.

It was noticed that the error in estimating slug length can be higher at a high gas flow rate; where Taylor bubbles are distorted and it becomes difficult to distinguish between the Taylor bubble and the wake zone within the liquid slug due to the increase in dispersed gas concentration within the liquid slug.

4.5.2 Slug Frequency

The frequency of the slug was estimated using the modified method of Hazuku et al. (2008) for large structures as detailed in section3. The results were compared with the PSD method and good agreement was obtained. The frequency of liquid slugs was estimated at three different locations in the riser for all the liquid velocities considered. Figure 15 illustrates how the frequency of slugs varies along the riser. It is clear that the slug frequency decreases along the pipe and also with the increase of superficial gas velocity. It is generally agreed that bubbles behind short liquid slugs moves faster than the leading one and hence merging process occurs. In the riser, the slug and Taylor bubble length increase along the pipe due to the merge of two consecutive Taylor bubbles. Therefore, the frequency decreases in the axial direction. Figure 15 also shows that the differences in slug frequencies at the three locations grow smaller with

increasing gas superficial velocity indicating rapid development of the flow at higher gas flow rates.

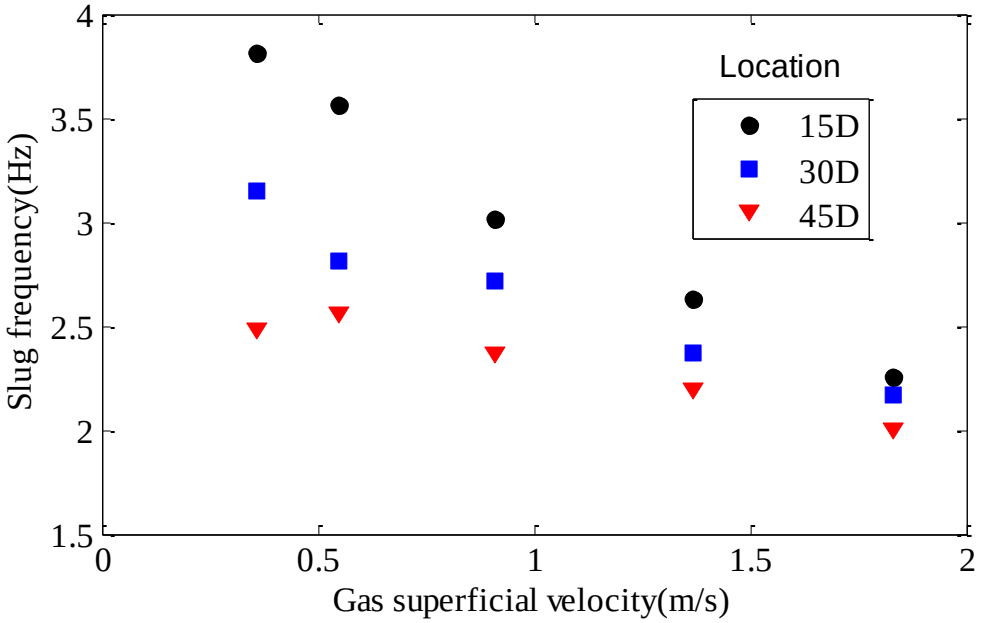

Figure 15: Frequency variation with increasing gas superficial velocity at three axial locations in the riser for constant liquid superficial velocity, U_{ls}=0.3ms^{-1}.

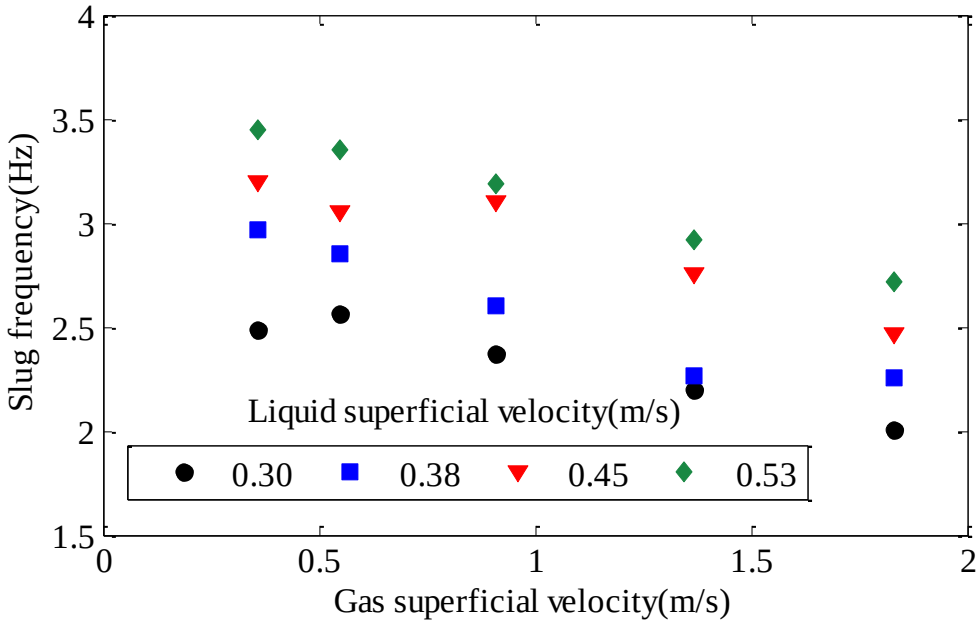

Figure 16: Slug frequency variation with air and oil superficial velocity in the riser.

Figure 16 shows the effect of the superficial liquid velocity on the frequency of the periodic structure of slugs at 45D. It can be clearly seen that the slug frequency increases with the increase of the superficial liquid velocity while continue to decrease with the increasing superficial gas velocity.

Several empirical correlations have been proposed to estimate the frequency of slugs, most of which are for horizontal or near horizontal flows. Some of the reported correlations**,** namely Sylvester (1987), Legius et al. (1997) and Zabaras (2000), were used to predict the frequency obtained experimentally as illustrated in Figure 17.

It is remarkable that Sylvester's (1987) correlation showed strong agreement with the experimental results. He presented a simple mathematical correlation given as Equation **Error! Reference source not found.** that requires the knowledge of slug unit velocity and length in order to predict the slug frequency.

$$f_s = \frac{U_{tb}(1-\beta)}{L_{ls}} \tag{8}$$

Slug unit velocity and the length are indicated by U_{tb} and L_{ls} respectively while β represents the ratio between the length of the Taylor bubble and the length of the slug unit. It should be noted that this equation need three independent variables to establish the slug frequency. Zabaras (2000) correlation has underestimated the experimental frequency. This is not surprising since, it is a modified version of Gregory and Scott (1969) correlation for horizontal flow, except that the effect of a small inclination up to 9 degrees was included. Legius et al. (1997) correlation has also dramatically under-predicted the experimental data. This clear discrepancy is due to the inherent limitation of this correlation. It is absolute replica of Heywood and Richardson (1979) correlation, for horizontal flow with a slightly modified constant.

It seems that most of the available correlations for predicting slug frequency in vertical flow are either mathematical models that include several unknown variables or simple empirical correlations that originally proposed for horizontal flow for a limited range of flow conditions. In order to develop a more general correlation, several parameters should be considered such as the physical properties of phases and pipe geometry in addition to the variables already considered.

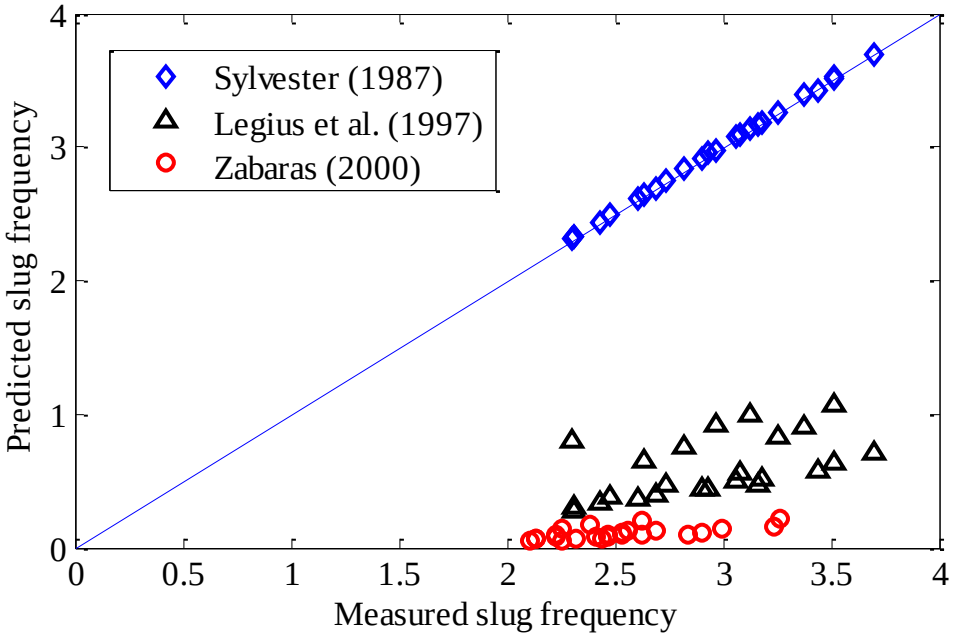

Figure 17: Comparison of the experimental slug frequency with the available correlation.

4.5.3 Void fraction in liquid slug

Void fraction in liquid slug (ε_{gSL}) is a crucial parameter in characterising slug flow which has a direct influence on the average void fraction. The knowledge of gas hold up within the body of the liquid slug has been considered as an input parameter for the several physical models developed to study slug flow such as Fernandes et al. (1983). It also can be used to determine the transition from slug to churn flow. In this work, the evolution of void fraction within the body of slugs was studied.

It is acknowledged that the gas phase is dynamically exchanged between the Taylor bubble and liquid slug. Gas bubbles at the rear of liquid slug coalesce with Taylor bubble while small bubbles are entrained into the liquid slug behind it due to the jet effect of the falling liquid film (Fernandes et al., 1983).

The liquid slug can be divided into three main regions based on the voidage profiles. The wake region which is a region of high turbulence and high local gas fraction, it extends to few pipe diameters downstream of the Taylor bubble. The translational region is an intermediate region that separates the wake and the developed region. The developed region starts at around 10D behind the Taylor bubble, It has a void fraction profile similar to that of dispersed bubbly flow (Van Hout et al., 1992).

Figure 18 illustrates the change in ε_{gSL} at three axial positions 15D, 30D and 45D downstream of the mixing section. The figure shows no significant change along the axial direction, particularly between 30D and 45D, however, it is clear that the averaged ε_{gSL} at 15D is slightly higher than the other two axial locations. This is more likely due to the nature of the flow near the entrance being more chaotic where slugs are still developing. The wake region within liquid slug is expected to be longer at this location and hence the overall gas holdup. It should also be noted that with increasing gas superficial velocity the gas hold up is higher in the silicon oil slugs.

The effect of liquid superficial velocity on the void fraction in liquid slugs is shown in Figure 19. Void fraction in the liquid slug follows the same trend discussed under Figure 18. However, it should be noted that with the increase of the liquid superficial velocity, the void fraction within the liquid slug decreases as shown in Figure 19. Similar observation is reported by other researchers (Akagawa and Sakaguchi, 1966; Barnea and Shemer, 1989; and Mori et al., 1999).

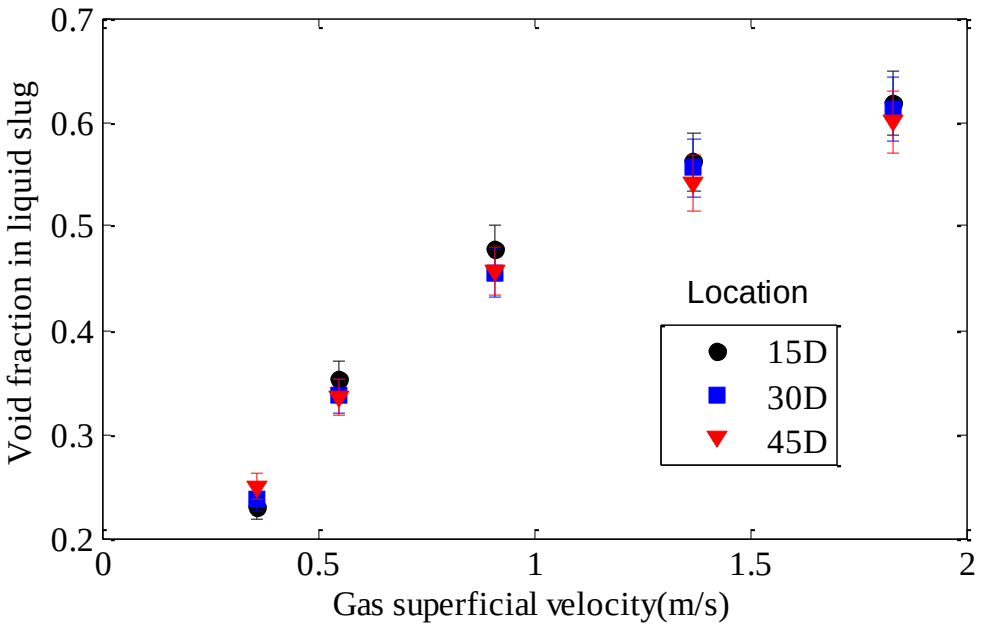

Figure 18: Void fraction in the liquid slug with increasing gas superficial velocity at three axial locations downstream of the gas injection point.

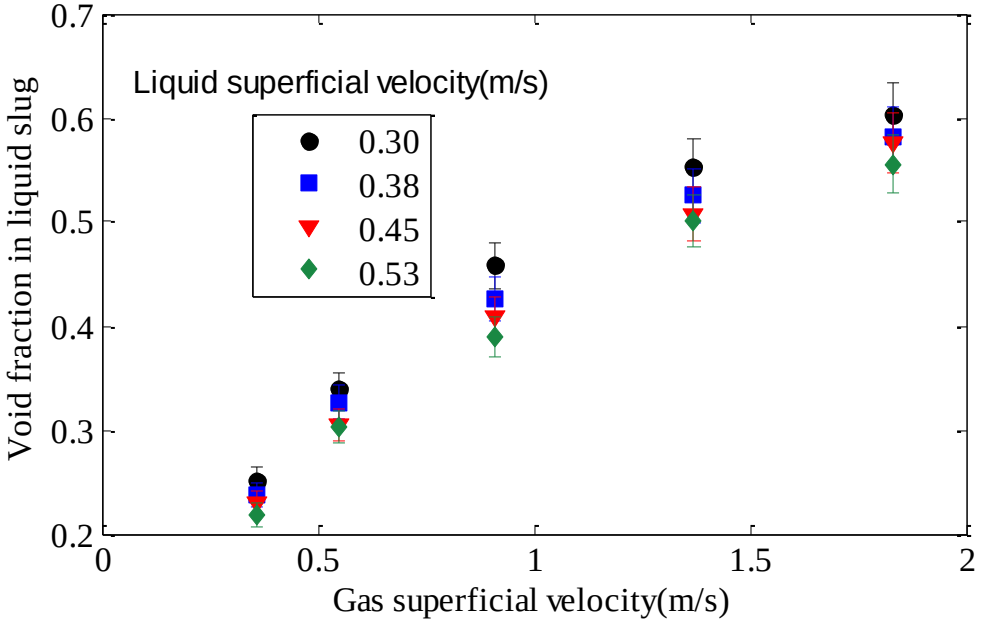

Figure 19: Effect of superficial gas velocity on the void fraction within the body of slugs.

It is expected that at high gas flow rate, the turbulence becomes dominant and hence more air is entrained into liquid slugs as a fine dispersion of bubbles. The averaged void fraction within the liquid slug varied from 0.23 to 0.63 over the range of the gas superficial velocities used in

this investigation. The lower value corresponds to the transition border for the bubbly flow while the higher value corresponds to the transition border for churn flow. Similar observation reported by Barnea and Shemer (1989). The lower value of 0.23 is almost equal to the suggested value of bubbly to slug transition (0.25) by Taitel et al. (1980). The upper value of 0.63 represents the maximum packing of bubbles in the liquid slug, hence the transition from slug to churn flow as suggested by Brauner and Barnea (1986).

It is acceptable that the liquid slugs can be treated as fully developed bubbly flow. Therefore liquid slugs can only accommodate maximum gas fraction equal to that of fully developed bubbly flow (Barnea and Brauner, 1985). Barnea and Shemer (1989), for air-water flow in 50mm ID pipe, reported that the void fraction in the liquid slug was 0.25 for U_{gs} below 1 $m.s^{-1}$. Beyond U_{gs} = 1 $m.s^{-1}$ the void fraction increased up to 0.6 which was considered the upper limit before the onset of the churn flow. Schmidt (1977) indicated that the void fraction in liquid slug varies from 0.2 to 0.8 for a wide range of U_{gs} and U_{ls} for air and kerosene mixture in 50 mm ID pipe.

In this work, the voidage in liquid slug continuously increases for the whole range of U_{gs} in slug flow region, and hence it eventually exceeds the value suggested for fully developed bubbly flow by Barnea and Brauner (1985). This behaviour is similar to Schmidt's (1977) observation for the air-kerosene system. It appears that void fraction in liquid slug is constant, i.e. can be equal to the value of dispersed bubbly flow, only for a limited range of superficial gas velocities. Beyond a critical value of $U_{gs,}$ the air entrainment in the body of the slug increases until slug/churn transition occurs. This value of U_{gs} might vary for different pipe configuration and flow conditions. Silicone oil has the ability entrain more bubbles in comparison to water. This can be confirmed by the observation of Schmidt (1977) for air-kerosene system which showed a continuous increase in the void fraction of liquid slugs. Pipe

diameter may also have an effect on slug characteristics since slugs appear more aerated in large pipes.

Figure 20 illustrates the predicted value of void fraction of liquid slugs by the available correlations reported in the literature, namely; Akagawa and Sakaguchi (1966), Sylvester (1987) and Mori et al. (1999) as shown respectively in the following equations:

$$\varepsilon_{gsl} = \varepsilon_g^{1.8} \tag{9}$$

$$\varepsilon_{gSL} = \frac{u_{gs}}{C_2 + C_3(u_{gs}+u_{ls})} \tag{10}$$

Where C_2 =0.425 and $C_3 = 2.65$

$$\varepsilon_{gsl} = 0.523\varepsilon_g \tag{11}$$

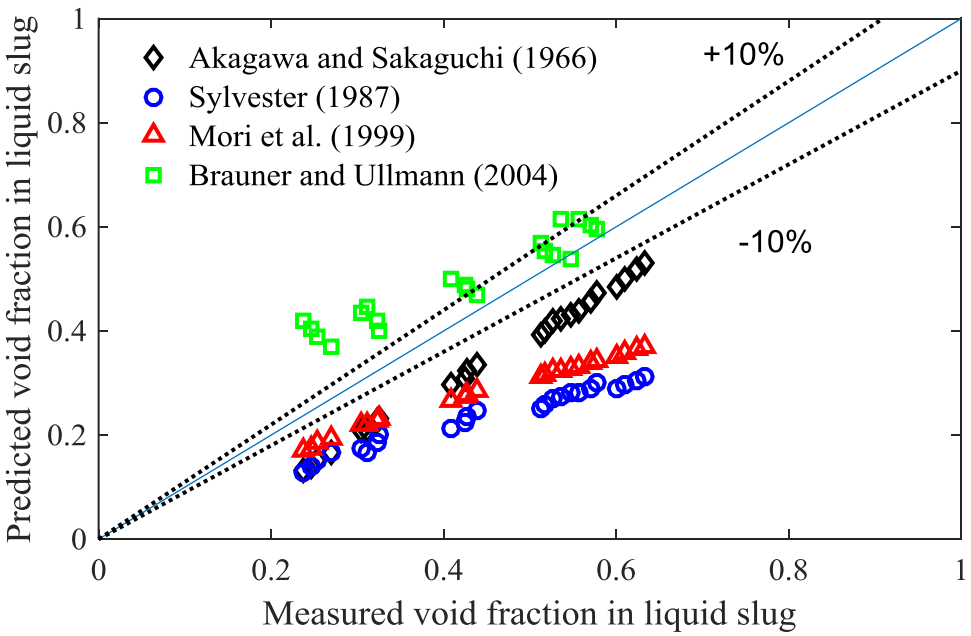

Figure 20: Comparison of void fraction in liquid slugs with empirical correlations.

The theoretical model of Brauner and Ullmann (2004), which is named as TBW model, was also used to predict the gas holdup in liquid slugs. It is clear that Brauner and Ullmann (2004) model gives the best estimation of void fraction in the body of the slugs with an average

absolute error of 24.05% and standard deviation of 1.03. The TBW model is theoretically derived and it is based on energy balance at the wake of Taylor bubble. Although it overpredicts the void fraction in liquid slugs, it seems to provide good estimation at high gas flowrates. Most of the estimated data, using TBW model, fall within 10% error margin.

Akagawa and Sakaguchi (1966) correlation underpredicts the experimental results with an average absolute error of 26.05% and standard deviation of 1.38. Correlations of Sylvester (1987) and Mori et al. (1999) showed larger drift from the experimental results with an average absolute error of 46.6% and 47.7% respectively. In fact, this was not surprising since correlations **Error! Reference source not found.** and **Error! Reference source not found.** were pure empirical fits for experimental results that were obtained for air-water system at pipes with smaller diameters (27.6mm ID and 25.8mmID). The equation **Error! Reference source not found.** was theoretically derived while the constants of the equation are based on the experimental work of Fernandes (1981). It is obvious that the silicone oil has a higher tendency to entrain more gas bubbles than water, especially at the high gas superficial velocities. These two empirical models predict the void fraction in liquid slugs closer to the measured values at low superficial gas velocity and continuously deviate as U_{gs} increases. However the model by Akagawa and Sakaguchi (1966) given in equation **Error! Reference source not found.** showed a consistent prediction for the whole range of gas superficial velocities used in our experiments. The performance of Akagawa and Sakaguchi correlation can be significantly improved if the exponent is set to 1.3 instead of 1.8**.** The prediction of the improved constant was in perfect agreement with the current experimental results with averaged absolute error of 2.02% and averaged standard deviation of 0.43. This suggests that this exponent would be a function of pipe diameter and the physical properties of the fluids. However, to establish such a relationship data for widely varied pipe geometries and fluid pairs are required.

It seems that there is no general correlation that predicts the void fraction within the liquid slugs for a wide range of operating conditions. Most of the available correlations were simple fits of experimental data for a limited range of operating conditions. Theoretical models such as Brauner and Ullmann (2004) seems to offer better prediction than any other experimental semiempirical correlations. Therefore, it can be said that the collective effect of different flow parameters such as pipe diameter and fluid properties should be carefully considered in order to develop more robust theoretical models.

4.5.4 Taylor bubble velocity

The Signals from the dual plane ECT sensor were cross-correlated to estimate the time delay of slugs between the sensor planes. The velocity is simply equal to the distance between the two planes divided by the time delay. The slug velocity was measured at three axial locations along the riser, in order to see how the axial velocity influences the evolution of slugs.

Figure 21 demonstrates the difference in the slug velocity in the axial direction. It can clearly be seen that the velocity increases with the increase of superficial gas velocity. It also increases in the axial direction under constant superficial gas velocities. This increase is significant from the first (15D) to the second location (30D), whereas at the third location (45D) the slug velocity showed only a small increase over that of 30D. This is due to the increase of bubble size as a subsequent merging process between two slug units since larger bubbles travel faster. The slugs are more stabilised at 45D location, where velocity profile within the slug unit is expected to be fully developed.

In addition, the change in static head with height can also enhance the velocity of Taylor bubbles. The effect of the gas and liquid superficial velocities on the slug unit at 45D downstream of the mixing section is presented in the Figure 22. It shows, as expected, an increase in structure velocity of the slugs with the increase in both, the gas and the liquid

superficial velocities. In these experiments, it was assumed that both the slug and the Taylor bubble are traveling at the same velocity. However, in reality, the Taylor bubble and liquid slug may travel at different velocities, which is usually considered to be small and has a negligible effect since the gas entrainment into and out of the Taylor bubble should be equal (Fernandes et al., 1983). It is noticeable that the superficial liquid velocity has a weaker effect on the slug velocity in comparison to that of the superficial gas velocity.

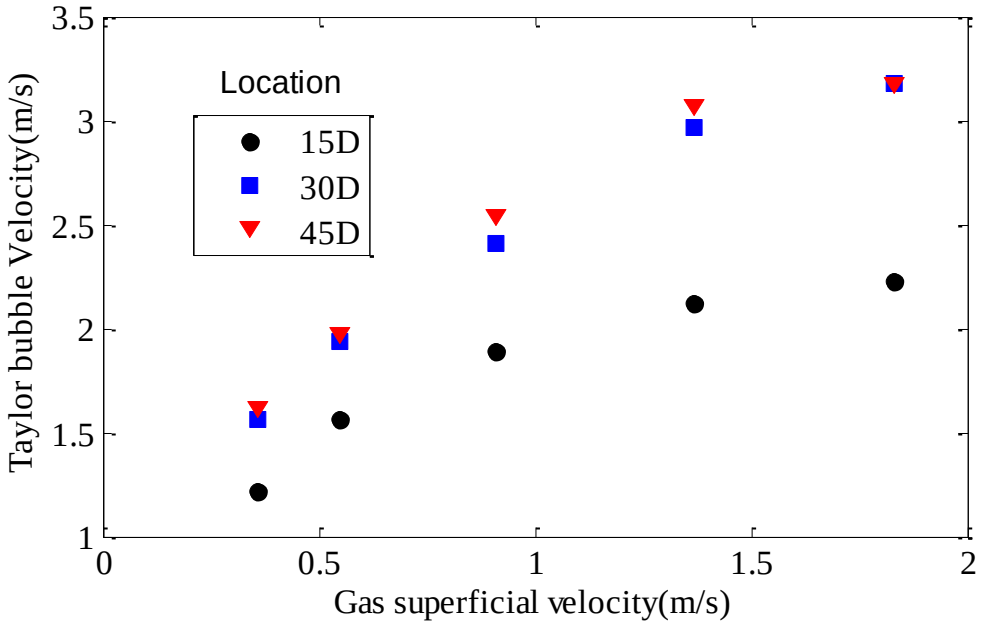

Figure 21: Taylor bubble velocity variation as a function of the axial distance in the riser at liquid superficial velocity = 0.3 ms^{-1}.

Taylor bubble velocity has been investigated extensively over years. The transitional velocity is considered to be a combination of the slug mixture velocity and the velocity of a bubble in a stagnant liquid, namely drift velocity and Nicklin et al. (1962) has suggested the following expression for the velocity of the Taylor bubble.

$$u_{gTB} = C_0\left(u_{gs} + u_{ls}\right) + U_d \qquad (12)$$

Where; U_d is the drift velocity given by equation **Error! Reference source not found.** and C_0 is the distribution parameter. C_0 is equal to the relative maximum velocity at the nose of the

bubble to the mixture velocity(U_{max}/U_m). It has been found to vary from 1.2 (Nicklin et al., 1962) to 1.29 (Fernandes et al., 1983) for developed slug flow.

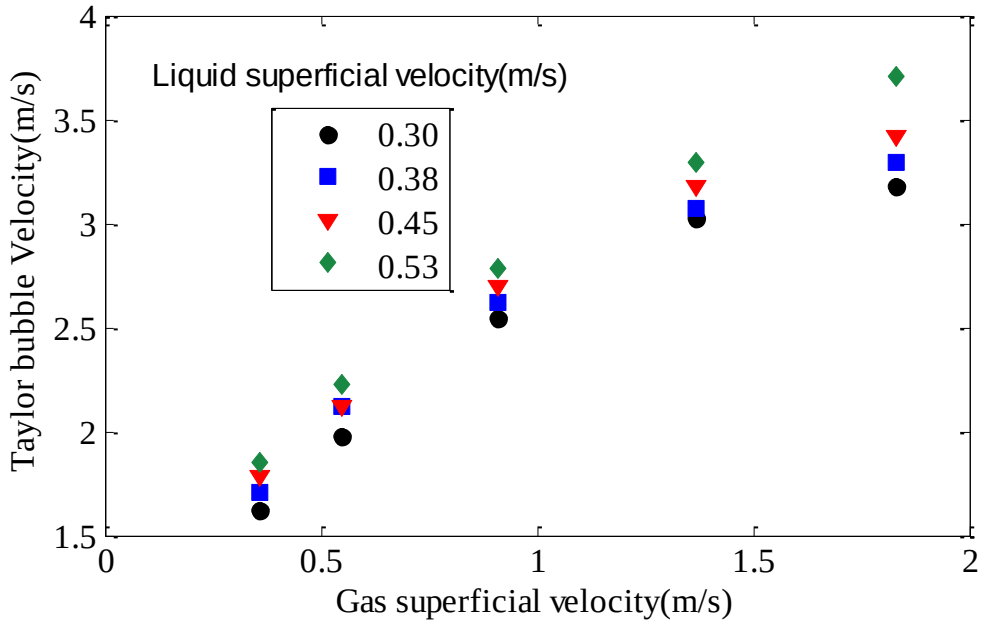

Figure 22: Taylor bubble velocity variation at 45D downstream of the mixer.

Figure 23 illustrates the comparison between the experimental and the estimated values of Taylor bubble velocity. The results are within an acceptable agreement. Taylor bubble velocity is underestimated by Nicklin et al. (1962) correlation with an average absolute error of 17.12% and standard deviation of 2.07. The discrepancy is more likely to be attributed to the effect of entrained bubbles within the liquid slug.

The rise velocity of Taylor bubble increases in the presence of bubbles in liquid slug (Mao and Dukler, 1985). It is evident that at the high superficial gas velocity, the Taylor bubble velocity is closely predicted. This could be a result of high gas entrainment in liquid slugs at these conditions. Mao and Dukler (1985) correlation has slightly improved the velocity prediction at low gas superficial velocity since it takes into consideration the effect of entrained bubbles on the transitional velocity of Taylor bubble. However, it overestimated the rise velocity

significantly at high gas flow. This is possibly due to the overcompensation of dispersed bubbles effect at high gas superficial velocity.

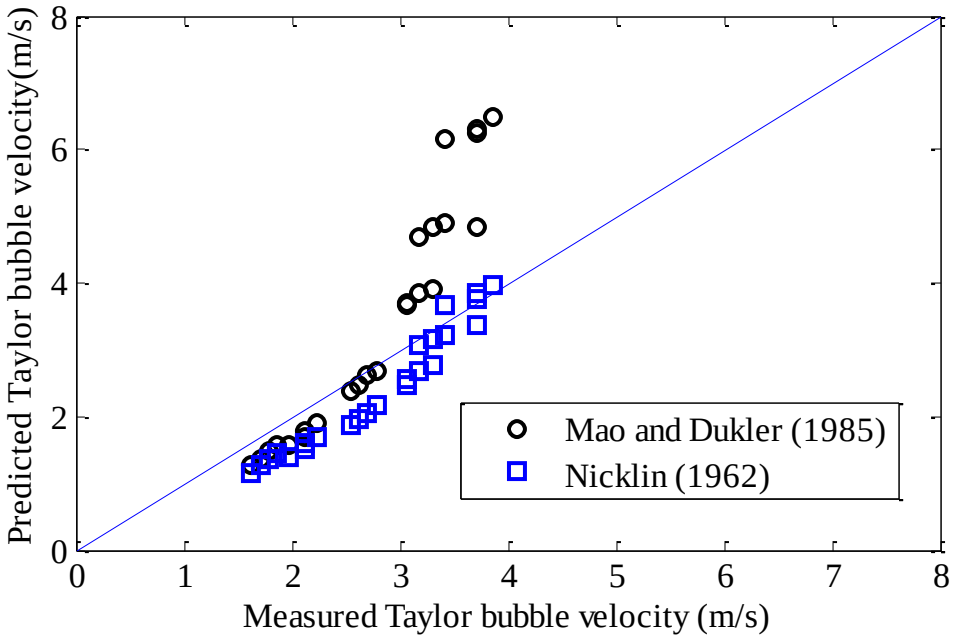

Figure 23: Experimental Taylor bubble velocity against the predicted values.

It could be thought that at the low superficial gas velocity, the entrained bubbles in liquid slugs are relatively large to flow down in the liquid film. Thus, these bubbles will merge with the front of Taylor bubble causing an increase in the rise velocity of Taylor bubble. As the gas superficial velocity increases, the gas holdup within the slug body increases. In this case, a swarm of tiny bubbles is entrained, and the liquid slug can be treated as a turbulent bubbly flow in which buoyancy decreases with the increase of void fraction as reported by Zuber and Hench (1962). The relative velocity of the entrained bubbles in the liquid is negligible; therefore the effect of entrained bubbles on the Taylor bubble velocity is expected to be negligible.

It must be mentioned that the distribution parameter (C_0) is highly dependent on the flow patterns and is a function of the inclination angle as well as other parameters, such as pipe diameter and mixture velocity. It is expected to increase with pipe diameter due to the effect of

gas expansion as reported by Fernandes et al. (1983). Therefore in the current study, the value 1.3 showed better prediction than the common value of 1.2.

4.6 Conclusion

Experiments in a 68mm ID vertical riser section are conducted using air-silicone oil mixture. Wire Mesh Sensor (WMS) and Electrical Capacitance Tomography (ECT) were used to provide cross-sectional averaged void fraction at three locations downstream of the mixing section. The experimental results were then compared to the predicted values of the available correlations. The key findings are concluded below:

- The flow structure showed an insignificant change between 45D and 65 D downstream of the mixing section, particularly at high gas superficial velocities. The liquid slugs are almost developed at 45 pipe diameter length, regardless the infrequent appearance of short slugs. It could be argued that the change in the flow structure may continue in extremely long pipes, due to the energy dissipation and pressure difference, however, this variation would be small on average.
- Developed slug flow occurs in vertical 68 mm ID pipes for gas superficial velocities between 0.36 $m.s^{-1}$ and 1.83 $m.s^{-1}$ and liquid superficial velocities up to 0.53 $m.s^{-1}$.
- Slug length increases in the axial direction and with the rise of gas superficial velocity. This increase is due to the emerging process between two consecutive slug units.
- The frequency of liquid slugs decreases along the axial direction and with the increase in gas superficial velocity. The reduction of slug frequency is due to slug coalescence.
- Void fraction within the liquid slug continuously increases with the increase of U_{gs}. The lowest and highest value within slug flow range corresponds to the transition from bubble to slug and from slug to churn respectively. Silicone oil seems to have higher void fraction than water, due to the difference in physical properties such as viscosity and surface tension.

- Taylor bubble tends to accelerate with the increase in superficial gas velocity and rise in the height of the vertical pipe. This is mainly due to the emerging process of two slug units, in addition to gas expansion and decrease in pressure with altitude.
- The available correlations for gas-liquid flow in vertical pipes are essentially based on air-water experiments. Most of them are empirical correlations that were developed by simply data fitting for a limited range of flow rates. Therefore the accuracy of these available models was diverse. The statistical performance comparison of the two-phase flow correlations used in this paper is presented in Table 1.

Table 1: The statistical analysis of the applied two-phase flow correlations

Source; Correlation	Pipe (ID); Fluids	Statistical measures		
		APE	AAPE	SD
Nicklin et al. (1962) $\varepsilon_d = \frac{U_{gs}}{C_0 U_m + U_d}$	26mm air/water	-2.37	2.88	0.58
Khatib and Richardson (1984) $L_S = \frac{C_0 U_m + U_0}{f_S}\left[\frac{\varepsilon - \varepsilon_{gTB}}{\varepsilon_{gsl} - \varepsilon_{gTB}}\right]$	38.8mm air/water air/slurry	-15.58	16.85	2.09
Sylvester (1987) $f_s = \frac{U_{tb}(1-\beta)}{L_{ls}}$	25mm to 75mm gas/water gas/oil	0.34	0.37	0.05
Zabaras (2000) $f_s = 0.0226\left[\frac{u_{sl}}{gd}\left(\frac{212.6}{u_m} + u_m\right)\right]^{1.2}[0.836 + 2.75\sin(\Theta)]$	25mm, 100mm air/water	-95.82	95.82	0.24
Legius et al. (1997) $f_s = 0.0543\frac{u_{ls}}{u_m}\left(\frac{2.02}{D} + \frac{u_m^2}{gD}\right)^{1.02}$	50mm air/water	-79.84	79.84	1.23
Akagawa and Sakaguchi (1966), $\varepsilon_{gsl} = \varepsilon_g^{1.8}$	27.6 mm air/water	-47.65	47.65	2.34
Sylvester (1987) $\varepsilon_{gSL} = \frac{u_{gs}}{C_2 + C_3(u_{gs} + u_{ls})}$	25mm to 75mm gas/water gas/oil	-46.59	46.60	0.72
Mori et al. (1999) $\varepsilon_{gsl} = 0.523\varepsilon_g$	25.8mm air/water	-47.70	47.70	0
Nicklin (1962) $u_{gTB} = C_0(u_{gs} + u_{ls}) + U_d$	26mm air/water	-15.86	17.11	2.07
Mao and Dukler (1985) $u_{gTB} = [(C_0 - \Phi)(u_m - U_o\varepsilon_{gSL} + U_d - U_o\Phi)](1-\Phi)^{-1}$	50mm air/water	15.46	28.99	6.04

References

Abdulkadir, M., Zhao, D., Azzi, A., Lowndes, I. S. & Azzopardi, B. J. (2012). Two-phase air–water flow through a large diameter vertical 180° return bend. *Chemical Engineering Science,* **79**, 138-152.

Akagawa, K. & Sakaguchi, T. (1966). Fluctuation of Void Ratio in Two-Phase Flow : 2nd Report, Analysis of Flow Configuration Considering the Existence of Small Bubbles in Liquid Slugs. *Bulletin of JSME,* **9**, 104-110.

Azzi, A. & Friedel, L. (2005). Two-phase upward flow 90° bend pressure loss model. *Forschung im Ingenieurwesen,* **69**, 120-130.

Azzopardi, B. J., Abdulkareem, L. A., Zhao, D., Thiele, S., da Silva, M. J., Beyer, M. & Hunt, A. (2010). Comparison between Electrical Capacitance Tomography and Wire Mesh Sensor Output for Air/Silicone Oil Flow in a Vertical Pipe. *Industrial & Engineering Chemistry Research,* **49**, 8805-8811.

Banowski, M., Beyer, M., Szalinski, L., Lucas, D. & Hampel, U. (2016). Comparative study of ultrafast X-ray tomography and wire-mesh sensors for vertical gas-liquid pipe flows. *Flow Measurement and Instrumentation*.

Barnea, D. & Brauner, N. (1985). Holdup of the liquid slug in two phase intermittent flow. *International Journal of Multiphase Flow,* **11**, 43-49.

Barnea, D. & Shemer, L. (1989). Void fraction measurements in vertical slug flow: applications to slug characteristics and transition. *International Journal of Multiphase Flow,* **15**, 495-504.

Benbella, S., Al-Shannag, M. & Al-Anber, Z. A. (2009). Gas–liquid pressure drop in vertical internally wavy 90° bend. *Experimental Thermal and Fluid Science,* **33**, 340-347.

Bendat, J. S. & Piersol, A. G. (1980). *Engineering applications of correlation and spectral analysis.*

Brauner, N. & Barnea, D. (1986). Slug/Churn transition in upward gas-liquid flow. *Chemical Engineering Science,* **41**, 159-163.

Brauner, N. & Ullmann, A. (2004). Modelling of gas entrainment from Taylor bubbles. Part A: Slug flow. *International Journal of Multiphase Flow,* **30**, 239-272.

Costigan, G. & Whalley, P. B. (1997). Slug flow regime identification from dynamic void fraction measurements in vertical air-water flows. *International Journal of Multiphase Flow,* **23**, 263-282.

Da Silva, M., Schleicher, E. & Hampel, U. (2007). Capacitance wire-mesh sensor for fast measurement of phase fraction distributions. *Measurement Science and Technology,* **18**, 2245.

Davies, R. M. & Taylor, G. (1950). The Mechanics of Large Bubbles Rising through Extended Liquids and through Liquids in Tubes. *Proceedings of the Royal Society of London A: Mathematical, Physical and Engineering Sciences,* **200**, 375-390.

Dumitrescu, D. T. (1943). Strömung an einer Luftblase im senkrechten Rohr. *ZAMM - Journal of Applied Mathematics and Mechanics / Zeitschrift für Angewandte Mathematik und Mechanik,* **23**, 139-149.

Fabre, J. (2003). Gas-Liquid Slug Flow. *In:* Bertola, V. (ed.) *Modelling and Experimentation in Two-Phase Flow.* Springer Vienna.

Fernandes, R. C. (1981). *Experimental and theoretical studies of isothermal upward gas-liquid flows in vertical tubes.* PhD, University of Houston.

Fernandes, R. C., Semiat, R. & Dukler, A. E. (1983). Hydrodynamic model for gas-liquid slug flow in vertical tubes. *AIChE Journal,* **29**, 981-989.

Gregory, G. A. & Scott, D. S. (1969). Correlation of liquid slug velocity and frequency in horizontal cocurrent gas-liquid slug flow. *AIChE Journal,* **15**, 933-935.

Hammer, E. A. (1983). *Three-component flow measurement in oil/gas/water mixtures using capacitance transducers.* PhD, University of Manchester.

Hazuku, T., Takamasa, T. & Matsumoto, Y. (2008). Experimental study on axial development of liquid film in vertical upward annular two-phase flow. *International Journal of Multiphase Flow,* **34**, 111-127.

Heywood, N. I. & Richardson, J. F. (1979). Slug flow of air—water mixtures in a horizontal pipe: Determination of liquid holdup by γ-ray absorption. *Chemical Engineering Science,* **34**, 17-30.

Hibiki, T. & Ishii, M. (2003). One-dimensional drift-flux model and constitutive equations for relative motion between phases in various two-phase flow regimes. *International Journal of Heat and Mass Transfer,* **46**, 4935-4948.

Huang, S. (1986). *Capacitance transducers for concentration measurement in multi-component flow processes.* University of Manchester, Institute of Science and Technology.

Ishii, M. (1977). One-Dimensional Drift-Flux Model and Constitutive Equations for Relative Motion between Phases in Various Two-Phase Flow Regimes. USA, Argonne National Lab.

Ito, D., Prasser, H. M., Kikura, H. & Aritomi, M. (2011). Uncertainty and intrusiveness of three-layer wire-mesh sensor. *Flow Measurement and Instrumentation,* **22**, 249-256.

Jones, O. C. & Zuber, N. (1975). The interrelation between void fraction fluctuations and flow patterns in two-phase flow. *International Journal of Multiphase Flow,* **2**, 273-306.

Khatib, Z. & Richardson, J. (1984). Vertical co-current flow of air and shear thinning suspensions of kaolin. *Chemical engineering research and design,* **62**, 139-154.

Legius, H. J. W. M., van den Akker, H. E. A. & Narumo, T. (1997). Measurements on wave propagation and bubble and slug velocities in cocurrent upward two-phase flow. *Experimental Thermal and Fluid Science,* **15**, 267-278.

Lucas, D., Krepper, E. & Prasser, H. M. (2005). Development of co-current air–water flow in a vertical pipe. *International Journal of Multiphase Flow,* **31**, 1304-1328.

Mao, Z.-S. & Dukler, A. E. (1985). Rise velocity of a Taylor bubble in a train of such bubbles in a flowing liquid. *Chemical Engineering Science,* **40**, 2158-2160.

Moissis, R. & Griffith, P. (1962). Entrance Effects in a Two-Phase Slug Flow. *Journal of Heat Transfer,* **84**, 29-38.

Mori, K., Kaji, M., Miwa, M. & Sekoguchi, K. (1999). Interfacial structure and void fraction of liquid slug for upward gas–liquid two-phase slug flow. *Two Phase Flow Modelling and Experimentation. Edizioni ETS, Pisa*.

Nicklin, D. J., Wilkes, J. O. & Davidson, J. F. (1962). Two-phase flow in vertical tubes. *Transaction of Institution of Chemical Engineers,* **40**, 61-68.

Nydal, O. J., Pintus, S. & Andreussi, P. (1992). Statistical characterization of slug flow in horizontal pipes. *International Journal of Multiphase Flow,* **18**, 439-453.

Prasser, H.-M., Krepper, E. & Lucas, D. (2002). Evolution of the two-phase flow in a vertical tube—decomposition of gas fraction profiles according to bubble size classes using wire-mesh sensors. *International Journal of Thermal Sciences,* **41**, 17-28.

Prasser, H. (Year). High-speed measurement of the void fraction distribution in ducts by wire-mesh sensors. *In:* International Meeting on Reactor Noise, 2000.

Prasser, H. M., Böttger, A. & Zschau, J. (1998). A new electrode-mesh tomograph for gas–liquid flows. *Flow Measurement and Instrumentation,* **9**, 111-119.

Prasser, H. M., Misawa, M. & Tiseanu, I. (2005). Comparison between wire-mesh sensor and ultra-fast X-ray tomograph for an air–water flow in a vertical pipe. *Flow Measurement and Instrumentation,* **16**, 73-83.

Prasser, H. M., Scholz, D. & Zippe, C. (2001). Bubble size measurement using wire-mesh sensors. *Flow Measurement and Instrumentation,* **12**, 299-312.

Schmidt, Ž. (1977). *Experimental study of two-phase slug flow in a pipeline-riser pipe system.* PhD, University of Tulsa,.

Sharaf, S., Da Silva, M., Hampel, U., Zippe, C., Beyer, M. & Azzopardi, B. (2011). Comparison between wire mesh sensor and gamma densitometry void measurements in two-phase flows. *Measurement Science and Technology,* **22**, 104019.

Sylvester, N. (1987). A mechanistic model for two-phase vertical slug flow in pipes. *Journal of energy resources technology,* **109**, 206-213.

Taitel, Y. & Barnea, D. (1990). Two-phase slug flow. *Advances in heat transfer,* **20**, 83-132.

Taitel, Y., Bornea, D. & Dukler, A. (1980). Modelling flow pattern transitions for steady upward gas-liquid flow in vertical tubes. *AIChE Journal,* **26**, 345-354.

Tomiyama, A. (1998). Struggle with computational bubble dynamics. *Multiphase Science and Technology,* **10**, 369-405.

Van Hout, R., Shemer, L. & Barnea, D. (1992). Spatial distribution of void fraction within a liquid slug and some other related slug parameters. *International Journal of Multiphase Flow,* **18**, 831-845.

Wallis, G. B. (1969). *One-dimensional two-phase flow.* McGraw-Hill Companies.

Zabaras, G. (2000). Prediction of slug frequency for gas/liquid flows. *SPE Journal,* **5**, 252-258.

Zuber, N. & Findlay, J. A. (1965). Average Volumetric Concentration in Two-Phase Flow Systems. *Journal of Heat Transfer,* **87**, 453-468.

Zuber, N. & Hench, J. (1962). Steady state and transient void fraction of bubbling systems and their operating limits (Part I, Steady State Operation). *General Electric Report 62GL100*.